Iminopyridine Complexes of 3d Metals for Ethylene Polymerization: Comparative Structural Studies and Ligand Size Controlled Chain Termination

Franz A. R. Kaul,[†] Gerd T. Puchta,[‡] Guido D. Frey,[§] Eberhardt Herdtweck, and Wolfgang A. Herrmann*

Department Chemie, Lehrstuhl für Anorganische Chemie, Technische Universität München, Lichtenbergstrasse 4, D-85747 Garching, Germany

Received September 19, 2006

A variety of iron complexes bearing tridentate pyridine based ligands are presented as highly active precatalysts for the oligomerization and polymerization of ethene and propene. The ligands comprise two classes: the first class, where both ketone groups of the 2,6-diacetylpyridine are converted to imines to give symmetrical or unsymmetrical bis(imino)pyridines (NNN ligands; **1**−**4**, **8**, and **9**), and the second class, where only one keto function of the 2,6-diacetylpyridine is substituted by an imine to give monoiminoacetylpyridines (NNO or MIAP ligands; **5**−**7**). The NNN ligands have been reacted with $FeCl_2 \cdot 4H_2O$ to afford the corresponding metal complexes (**12**−**17**). These complexes have been activated by modified methylaluminoxane (MMAO) and tested in the oligomerization and polymerization reaction of ethene and propene. Depending on the steric bulk of the ortho substituents at the aryl group of the imines, tunable polymerization products are observed, with molecular weights (M_w) of 10^2-10^6. Using the MIAP ligands, complexes of Co(II), Cr(II), Fe(II), Mn(II), and Ni(II) (**18**−**24**) have been prepared. The solid-state X-ray structures of the square-pyramidal {2-acetyl-6-[1-((2,6-diisopropylphenyl)imino)-ethyl]pyridine}metal halide complexes **18**, **21**, and **22b** (M = Co(II), Fe(II), Ni(II)) have been compared. Additionally, the solid-state structure of {2,6-bis[1-(1-biphenylimino)ethyl]pyridine}iron(II) chloride (**15**) is presented. All ligands and complexes have been characterized by spectroscopic methods, mass spectra, and elemental analysis.

Introduction

Over the past 60 years few research areas have had as tremendous an impact on human civilization than tailor-made polyolefins. Initially discovered in the 1950s by Ziegler and Natta[1,2] and driven by the desire to improve the properties of polyolefinic materials, the design and the modification of useful organometallic or coordinate catalysts have been in sharp focus ever since. Introduced by traditional Ziegler−Natta catalysts which had the early transition metal titanium as the catalytically active center, much effort was involved using early transition metals when searching for new types of catalysts, of which metallocene and coordinate chromium-based catalysts have been intensely studied.[3] However, there was always great interest in the application of late transition metals as catalysts for the polyolefination of alkenes.[4] The Shell Higher Olefins Process (SHOP) was developed after screening new catalysts[5] and showed the potential of late-transition-metal catalysts for polymerization.[6] A revolutionary system was reported by Brookhart and co-workers, in which nickel(II) and palladium-(II) complexes containing bulky α-diimine ligands were capable of polymerizing ethylene to give high-molecular-weight polymers. These catalysts showed the important role of the synergy between stereo and electronic effects of the ligands and the catalytic activity of the metal center. Since the discovery in 1998 by Brookhart[7,8] and Gibson[9,10] that complexes of late transition metals, such as iron and cobalt, with bulky 2,6-bis(imino)-pyridine ligands[11,12] (NNN ligands) and their derivatives[13] were highly catalytically active for polyolefination,[14] the interest in polymerization catalysts other than metallocenes has greatly increased.[15−27]

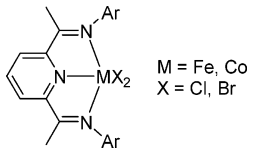

Because of their lower oxophilicity,[28] these "post-metallocene catalysts" are well-suited for applications in the copolymerization of α-olefins with polar monomers such as alkyl acry-

* To whom correspondence should be addressed. E-mail: lit@arthur.anorg.chemie.tu-muenchen.de.

† Present address: EPCOS AG, Anzingerstrasse 13, D-81617 München, Germany.

‡ Present address: Rehau AG & Co., Otto-Hahn-Strasse 2, 95111 Rehau, Germany.

§ Present address: UCR-CNRS Joint Research Chemistry Laboratory (UMI 2957), Department of Chemistry, University of California, Riverside, CA 92521-0403.

(1) Ziegler, K.; Holzkamp, E.; Breil, H.; Martin, H. *Angew. Chem.* **1955**, *67*, 541.

(2) Natta, G. *Angew. Chem.* **1956**, *68*, 393.

(3) (a) Brintzinger, H.-H.; Fischer, D.; Mülhaupt, R.; Rieger, B.; Waymouth, R. M. *Angew. Chem.* **1995**, *107*, 1255; *Angew. Chem., Int. Ed. Engl.* **1995**, *34*, 1143. (b) White, P. A.; Calabrese, J.; Theopold, K. H. *Organometallics* **1996**, *15*, 5473. (c) McKnight, A. L.; Waymouth, R. M. *Chem. Rev.* **1998**, *98*, 2587.

(4) Hartley, F. R. *Chem. Rev.* **1969**, *69*, 799.

(5) (a) Nieuwenhuis, R. A. *Pet. Tech.* **1980**, *268*, 46. (b) Spitzer, E. L. T. M. *Seifen, Oele, Fette, Wachse* **1981**, *107*, 141.

(6) (a) Ittle, S. D.; Johnson, L. K.; Brookhart, M. *Chem. Rev.* **2000**, *100*, 1169. (b) Britovsek, G. J. P.; Gibson, V. C.; Wass D. F. *Angew. Chem.* **1999**, *111*, 448; *Angew. Chem., Int. Ed.* **1999**, *38*, 428.

10.1021/om060857q CCC: $37.00
Publication on Web 01/11/2007

lates.[28,29] Due to problems (e.g., reactor fouling and an extremely exothermic polymerization process) arising from the homogeneous nature of the polymerization catalysts, the application of these polymerization catalysts in gas-phase or slurry reactions still is comparatively problematic.

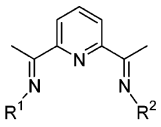

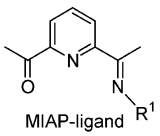

1: $R^1 = R^2$ = 2,6-diisopropylphenyl
2: $R^1 = R^2$ = 1-anthracenyl
3: $R^1 = R^2$ = 2-isopropylphenyl
4: $R^1 = R^2$ = 2-biphenyl
5: R^1 = 2,6-diisopropylphenyl
6: R^1 = 2-isopropylphenyl
7: R^1 = 2,6-dimethylphenyl
8: R^1 = 2,6-diisopropylphenyl, R^2 = 1-anthracenyl
9: R^1 = 2,6-diisopropylphenyl, R^2 = 2-isopropylphenyl

Figure 1. Synthesized iminopyridine compounds.

In this article, we report the synthesis of a series of bis(imino)-pyridine 3d metal complexes and their catalytic behavior for a chain-controlled ethylene and propylene polymerization according to the ligand size and steric effects. Reaction parameters, such as temperature and cocatalyst concentration, have also been investigated for their effect on polymerization activity.

Results and Discussion

The symmetrical NNN compounds **1**−**4** were synthesized from the reaction of 2,6-diacetylpyridine with the appropriate amines, similar to the procedure by Alt et al. (see Figure 1).[30] These compounds have already been described elsewhere (see refs 7, 9, 15, 30−32 and references therein).

The synthesis of monoiminoacetylpyridines (MIAP ligands) was carried out according to a known method.[30] In this case, the aniline derivatives were used in only 0.98 equiv amount in a protic solvent. Compound **5** could be recrystallized in 85% yield from a methanol solution at room temperature. Much lower temperatures (−30 °C) were necessary for compound **7**. Only compound **6** could not be obtained in high yields, because of its excellent solubility in methanol during recrystallization; for this reason, the compound was recrystallized from the less polar solvent ethanol in 53% yield. Another problem occurs during the preparation of compound **6**, where a high amount of the disubstituted byproduct **3** was obtained.

For the synthesis of unsymmetrical 2,6-bis(imino)pyridine compounds the compound **5** was used as the starting material. It is recommended to use an excess of the precursor **5**, if it is not possible to remove the aniline compound from the reaction mixture, as is the case for compound **8**. The excess of 2-isopropylaniline used for the preparation of compound **9** can be removed very easily by distillation.[16]

Syntheses of an Alkene-Functionalized Compound (10). With the 2,6-bis{1-[2,6-(diisopropylphenyl)imino]ethyl}pyridine compound **1** reported by Brookhart and Gibson as the starting

(7) (a) Small, B. L.; Brookhart, M.; Bennet, A. M. A. *J. Am. Chem. Soc.* **1998**, *120*, 4049. (b) Small, B. L.; Brookhart, M. *Macromolecules* **1999**, *32*, 2120.
(8) Small, B. L.; Brookhart, M. *J. Am. Chem. Soc.* **1998**, *120*, 7143.
(9) (a) Britovsek, G. J. P.; Gibson, V. C.; Kimberley, B. S.; Maddox, P. J.; McTavish, S. J.; Solan, G. A.; White, A. J. P.; Williams, D. J. *Chem. Commun.* **1998**, 849. (b) Britovsek, G. J. P.; Gibson, V. C.; Wass, D. F. *Angew. Chem.* **1999**, *111*, 448; *Angew. Chem., Int. Ed.* **1999**, *38*, 428.
(10) Britovsek, G. J. P.; Bruce, M.; Gibson, V. C.; Kimberley, B. S.; Maddox, P. J.; Mastroianni, S.; McTavish, S. J.; Redshaw, C.; Solan, G. A.; Strömberg, S.; White, A. J. P.; Williams, D. J. *J. Am. Chem. Soc.* **1999**, *121*, 8728.
(11) (a) Steffen, W.; Blömker, T.; Kleigrewe, N.; Kehr, G.; Fröhlich, R.; Erker, G. *Chem. Commun.* **2004**, 1188. (b) Lappalainen, K.; Yliheikkila, K.; Abu-Surrah, A. S.; Polamo, M.; Leskelä, M.; Repo, T. *Z. Anorg. Allg. Chem.* **2005**, *631*, 763. (c) Britovsek, G. J. P.; England, J.; Spitzmesser, S. K.; White, A. J. P.; Williams, D. J. *Dalton Trans.* **2005**, 945. (d) Bouwkamp, M. W.; Bart, S. C.; Hawrelak, E. J.; Trovitch, R. J.; Lobkovsky, E.; Chirik, P. J. *Chem. Commun.* **2005**, 3406. (e) Kleigrewe, N.; Steffen, W.; Blömker, T.; Kehr, G.; Fröhlich, R.; Wibbeling, B.; Erker, G.; Wasilke, J.-C.; Wu, G.; Bazan, G. C. *J. Am. Chem. Soc.* **2005**, *127*, 13955. (f) Scott, J.; Gambarotta, S.; Korobkov, I.; Knijnenburg, Q.; de Bruin, B.; Budzelaar, P. H. M. *J. Am. Chem. Soc.* **2005**, *127*, 17204. (g) Champouret, Y. D. M.; Marechal, J.-D.; Dadhiwala, I.; Fawcett, J.; Palmer, D.; Singh, K.; Solan, G. A. *Dalton Trans.* **2006**, 2350.
(12) Suhr, D.; Lötscher, D.; Stoeckli-Evans, H.; von Zelewsky, A. *Inorg. Chim. Acta* **2002**, *341*, 17.
(13) Britovsek, G. J. P.; Gibson, V. C.; Hoarau, O. D.; Spitzmesser, S. K.; White, A. J. P.; Williams, D. J. *Inorg. Chem.* **2003**, *42*, 3454.
(14) Britovsek, G. J. P.; Mastroianni, S.; Solan, G. A.; Baugh, S. P. D.; Redshaw, C.; Gibson, V. C.; White, A. J. P.; Williams, D. J.; Elsegood, M. R. J. *Chem. Eur. J.* **2000**, *6*, 2221.
(15) Benvenuti, F.; Francois, P. (Solvay Polyolefins Europe-Belgium) US 6670434 B2; US 2003/0018147 A1; BE 1014196 A3, 2003.
(16) Ma, Z.; Sun, W.-H.; Li, Z.-L.; Shao, C.-X.; Hu, Y.-L.; Li, X.-H. *Polym. Int.* **2002**, *51*, 994.
(17) Bianchini, C.; Giambastiani, G.; Guerrero, I. R.; Meli, A.; Passaglia, E.; Gragnoli, T. *Organometallics* **2004**, *23*, 6087.
(18) Liu, J.-Y.; Zheng, Y.; Li, Y.-G.; Pan, L.; Li, Y.-S.; Hu, N.-H. *J. Organomet. Chem.* **2005**, *690*, 1233.
(19) Scott, J.; Gambarotta, S.; Korobkov, I.; Budzelaar, P. H. M. *J. Am. Chem. Soc.* **2005**, *127*, 13019.
(20) (a) Souane, R.; Isel, F.; Peruch, F.; Lutz, P. J. *C. R. Chim.* **2002**, *5*, 43. (b) Chen, Y.-F.; Qian, C.-T.; Sun, J. *Organometallics* **2003**, *22*, 1231. (c) Chen, Y.-F.; Chen, R.-F.; Qian, C.-T.; Dong, X.-C.; Sun, J. *Organometallics* **2003**, *22*, 4312. (d) Castro, P. M.; Lappalainen, K.; Ahlgren, M.; Leskela, M.; Repo, T. *J. Polym. Sci., Part A: Polym. Chem.* **2003**, *41*, 1380. (e) Britovsek, G. J. P.; Baugh, S. P. D.; Hoarau, O.; Gibson, V. C.; Wass, D. F.; White, A. J. P.; Williams, D. J. *Inorg. Chim. Acta* **2003**, *345*, 279. (f) Paulino, I. S.; Schuchardt, U. *J. Mol. Catal. A: Chem.* **2004**, *211*, 55. (g) Zhang, Z.-C.; Chen, S.-T.; Zhang, X.-F.; Li, H.; Ke, Y.; Lu, Y.-Y.; Hu, Y.-L. *J. Mol. Catal. A: Chem.* **2005**, *230*, 1. (h) Pelascini, F.; Peruch, F.; Lutz, P. J.; Wesolek, M.; Kress, J. *Eur. Polym. J.* **2005**, *41*, 1288. (i) Calderazzo, F.; Englert, U.; Pampaloni, G.; Santi, R.; Sommazzi, A.; Zinna, M. *Dalton Trans.* **2005**, 914. (j) Yliheikkila, K.; Lappalainen, K.; Castro, P. M.; Ibrahim, K.; Abu-Surrah, A.; Leskelä, M.; Repo, T. *Eur. Polym. J.* **2006**, *42*, 92. (k) Ionkin, A. S.; Marshall, W. J.; Adelman, D. J.; Bobik-Fones, B.; Fish, B. M.; Schiffhauer, M. F. *Organometallics* **2006**, *25*, 2978. (l) Ionkin, A. S.; Marshall, W. J.; Adelman, D. J.; Shoe, A. L.; Spence, R. E.; Xie, T. *J. Polym. Sci., Part A: Polym. Chem.* **2006**, *44*, 2615. (m) Archer, A. M.; Bouwkamp, M. W.; Cortez, M.-P.; Lobkovsky, E.; Chirik, P. J. *Organometallics* **2006**, *25*, 4269.
(21) (a) Gibson, V. C.; McTavish, S.; Redshaw, C.; Solan, G. A.; White, A. J. P.; Williams, D. J. *Dalton Trans.* **2003**, 221. (b) Gibson, V. C.; Long, N. J.; Oxford, P. J.; White, A. J. P.; Williams, D. J. *Organometallics* **2006**, *25*, 1932.
(22) (a) Liu, J.-Y.; Li, Y.-S.; Liu, J.-Y.; Li, Z.-H. *Macromolecules* **2005**, *38*, 2559. (b) Overett, M. J.; Meijboom, R.; Moss, J. R. *Dalton Trans.* **2005**, 551.
(23) Abu-Surrah, A. S.; Lappalainen, K.; Piironen, U.; Lehmus, P.; Repo, T.; Leskelä, M. *J. Organomet. Chem.* **2002**, *648*, 55.
(24) O'Reilly, R. K.; Gibson, V. C.; White, A. J. P.; Williams, D. J. *Polyhedron* **2004**, *23*, 2921.
(25) (a) Qiu, J.-M.; Li, Y.-F.; Hu, Y.-L. *Polym. Int.* **2000**, *49*, 5. (b) Ma, Z.; Wang, H.; Qiu, J.-M.; Xu, D.; Hu, Y.-L. *Macromol. Rapid Commun.* **2001**, *22*, 1280.
(26) Esteruelas, M. A.; Lopez, A. M.; Mendez, L.; Olivan, M.; Onate, E. *Organometallics* **2003**, *22*, 395.
(27) (a) Babik, S. T.; Fink, G. *J. Mol. Catal. A: Chem.* **2002**, *188*, 245. (b) Bryliakov, K. P.; Semikolenova, N. V.; Zakharov, V. A.; Talsi, E. P. *Organometallics* **2004**, *23*, 5375. (c) Humphries, M. J.; Tellmann, K. P.; Gibson, V. C.; White, A. J. P.; Williams, D. J. *Organometallics* **2005**, *24*, 2039.
(28) Johnson, L. K.; Mecking, S.; Brookhart, M. *J. Am. Chem. Soc.* **1996**, *118*, 267.
(29) Younkin, T. R.; Connor, E. F.; Henderson, J. I.; Friedrich, S. K.; Grubbs, R. H.; Bansleben, D. A. *Science* **2000**, *287*, 460.
(30) (a) Schmidt, R.; Welch, M. B.; Palackal, S. J.; Alt, H. G. *J. Mol. Catal. A: Chem.* **2002**, *179*, 155. (b) Schmidt, R.; Welch, M. B.; Knudsen, R. D.; Gottfried, S.; Alt, H. G. *J. Mol. Catal. A: Chem.* **2004**, *222*, 9.
(31) Bennett, A. M. A. (E.I. DuPont De Nemours and Conpany) WO 98/27124, 1998; U.S. Patent 6063881, 2000; Eur. Patent EP 0946609 B1, 2002; Eur. Patent EP 1066229 B1, 2004.
(32) Hiya, K.; Nakayama, Y.; Yasuda, H. *Macromolecules* **2003**, *36*, 7916.

Scheme 1. Preparation of Unsymmetrical Bis(imino)pyridine Compounds

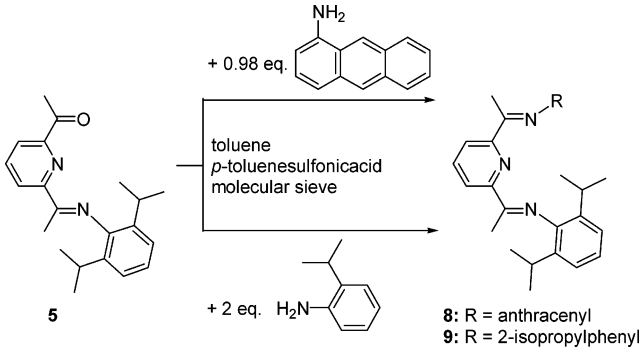

Scheme 2. Preparation of the Styrene-Substituted Complex 11

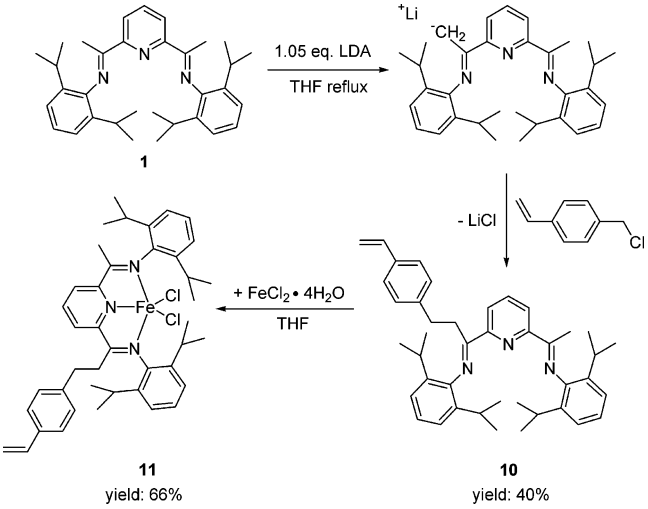

material,[7,9] the functionalization was achieved by deprotonation of the bis(imino)pyridine compound with lithium diisopropylamide. The yellow solution of compound **1** immediately turned dark green, almost black. After the mixture was kept under reflux for 12 h, 4-vinylbenzyl chloride was added and the mixture stirred for 5 days, affording **10** (Scheme 1). The reaction was finished when the solution turned red.

Complex Synthesis. [Bis(imino)pyridine]iron(II) complexes were synthesized according to published methods[7,9] by addition of $FeCl_2 \cdot 4H_2O$ to a stirred solution of the compounds **1**−**4** and **8**−**10** in *n*-BuOH or THF.[26] The resulting deep blue iron complexes **11**, **12**,[7,9] and **13**−**17** are depicted in Schemes 2 and 3. Blue crystals of complex **15** suitable for a single-crystal X-ray diffraction study were obtained by slow diffusion of diethyl ether into a saturated dichloromethane solution. The solid-state structure of the iron complex **15** is shown in Figure 2. Details of the data collection and refinement of the analysis are summarized in Table 3, and selected bond lengths and angles are presented in Table 2.

In comparison to the previously reported complex **12** by Gibson et al., where the 2,6-diisopropylphenyl groups are substituted at the bis(imino)pyridine complex (Fe−N = 2.238(4) and 2.250(4) Å),[9,14] complex **15** shows shorter Fe−N(2) and Fe−N(3) bond lengths (Fe−N = 2.195(1) and 2.182(1) Å). This is attributed to the decreased steric bulk of the substituents ortho to the imino groups. The slightly wider N(2)−Fe−N(3) angle (by 4°) is caused from the longer Fe−N bond length obtained in this complex. A square-pyramidal geometry was also found for complex **15** as well as for the 2,6-diisopropylphenyl-substituted complex **12**.

Scheme 3. Preparation of Bis(imino)pyridine-Substituted Iron(II) Complexes 12−17

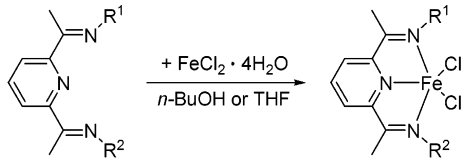

1, 12: R^1, R^2 = 2,6-diisopropylphenyl
2, 13: R^1, R^2 = 1-anthracenyl
3, 14: R^1, R^2 = 2-isopropylphenyl
4, 15: R^1, R^2 = 2-biphenyl
8, 16: R^1 = 2,6-diisopropylphenyl, R^2 = 1-anthracenyl
9, 17: R^1 = 2,6-diisopropylphenyl, R^2 = 2-isopropylphenyl

The unsymmetrical [bis(imino)pyridine]iron(II) complexes **16** and **17** can be perceived as hybrids of complexes **12**−**14** (Scheme 3). They were characterized, as were all other previously mentioned complexes, by MS, IR, and elemental analysis. We were not able to obtain crystals suitable for X-ray analysis from the complexes **16** and **17**. An explanation for the reluctance of complex **16** to crystallize could be its high solubility in many solvents, the unsymmetrical character of the complex, and probably the high rotation liberty of the isopropyl groups.

The styrene-substituted complex **11** was obtained from a THF/*n*-pentane solution in 66% yield, in the same way as for all other [bis(imino)pyridine]iron complexes (Scheme 2). This complex has the potential to be immobilized via the ligand's styrene moiety onto a polystyrene carrier.[33]

A series of [mono(imino)pyridine]metal(II) dihalide complexes, bearing hydrocarbon ligands (**5**−**7**), were prepared by using hydrated or dehydrated transition-metal salts such as $FeCl_2 \cdot 4H_2O$ and $CoCl_2$ in DCM (Scheme 4).[34] Using transition-metal complexes with a coordinated solvent such as (DME)-$NiBr_2$ increases the solubility in organic solvents and is of advantage during the synthesis.[35] The strong colors of the iron complex **18** (purple) and the cobalt complex **21** (green) can be explained by ligand field theory effects, such as those shown recently for [bis(imino)pyridine]metal complexes.[19,36] In contrast, complexes **20** and **22**−**24** are brown or ocher.

The complexes **18**−**24** were characterized by their elemental analysis, mass spectra, and infrared spectra. A comparison of the IR data for the C═O and C═N stretching frequencies shows a significant shift during the change from early to late transition metals in their oxidation state +II (Table 1). The strong shift to smaller wavenumbers of the Cr(II) complex **19** is striking. This can be explained by the highly oxophilic character of chromium, as a consequence of the increased Lewis acidity: in the HSAB concept, chromium(II) is a harder Lewis acid than the following periodic neighbors.[37] The C═O double-bond character is increased by the donor effect of the free electron pairs of the oxygen to the metal; consequently, a lower

(33) (a) Zheng, Z.-J.; Chen, J.; Li, Y.-S. *J. Organomet. Chem.* **2004**, *689*, 3040. (b) Zheng, Z.-J.; Liu, J.-Y.; Li, Y.-S. *J. Catal*. **2005**, *234*, 101. (c) Han, W.; Müller, C.; Vogt, D.; Niemantsverdriet, H. J. W.; Thüne, P. C. *Macromol. Rapid Commun.* **2006**, *27*, 279.

(34) For example: Fernandes, S.; Bellabarba, R. M.; Ribeiro, A. F. G.; Gomes, P. T.; Ascenso, J. R.; Mano, J. F.; Dias, A. R.; Marques, M. M. *Polym. Int.* **2002**, *51*, 1301.

(35) Bluhm, M. E.; Folli, C.; Döring, M. *J. Mol. Catal. A: Chem.* **2004**, *212*, 13.

(36) Small, B. L.; Carney, M. J.; Holman, D. M.; O'Rourke, C. E.; Halfen, J. A. *Macromolecules* **2004**, *37*, 4375.

(37) Muelhaupt, R. *Nachr. Chem. Tech. Lab.* **1993**, *41*, 1341.

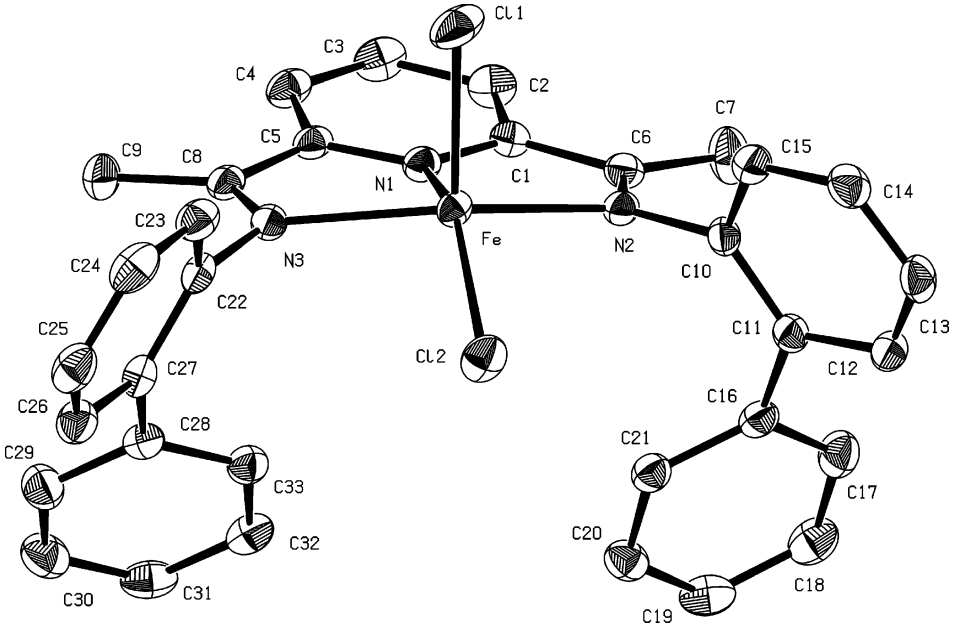

Figure 2. ORTEP style plot of complex **15** in the solid state. Thermal ellipsoids are drawn at the 50% probability level. Hydrogen atoms are omitted for clarity. Selected bond lengths (Å) and bond angles (deg) are given in Table 2.

Scheme 4. Preparation of [Mono(imino)pyridine]metal(II) Complexes

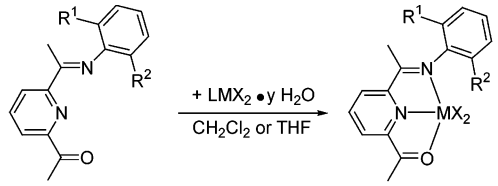

5: $R^1 = R^2 = i$-Pr
6: $R^1 = i$-Pr, R^1 = H
7: $R^1 = R^2$ = Me

M = Fe, Mn, Co, Ni
L = none, DME
X = Cl, Br
y = 0, 4, 6

18 - 24

	18	**19**	**20**	**21**	**22a**	**22b**	**23**	**24**
M	Fe	Cr	Mn	Co	Ni	Ni	Ni	Ni
R^1	*i*-Pr	*i*-Pr	*i*-Pr	*i*-Pr	*i*-Pr	*i*-Pr	Me	*i*-Pr
R^2	*i*-Pr	*i*-Pr	*i*-Pr	*i*-Pr	*i*-Pr	*i*-Pr	Me	H
X	Cl	Cl	Cl	Cl	Cl	Br	Br	Br
yield (%)	86	79	67	75	54	96	92	88

Table 1. Comparison of the *ν*(CO) and *ν*(CN) Absorption Frequencies (cm^{-1}) of Different 3d Metal Complexes

	5	**19** (Cr(II))	**20** (Mn(II))	**18** (Fe(II))	**21** (Co(II))	**22a** ($NiCl_2$)	**22b** ($NiBr_2$)	**6**	**24** ($NiBr_2$)	**7**	**23** ($NiBr_2$)
C═O	1698.6	1633.9	1676.6	1689.4	1675.9	1668.2	1673.3	1695.6	1666.5	1697.5	1667.6
C═N	1647.9	1577.9	1588.6	1588.4	1588.6	1588.6	1591.9	1647.6	1586.7	1586.7	1590.3

wavenumber (1633.9 cm^{-1}) is obtained (Table 1). For the C═N stretching frequency this effect is much more intense, because the free electron pair of the nitrogen is a much stronger donor (harder base) than oxygen. For this reason, a shift of nearly 70 cm^{-1} occurs compared to the free compound. For the following periodic neighbors, a shift for the C═N stretching frequency of around 60 cm^{-1} was obtained. The variation of the C═O stretching frequency might also be influenced by some geometric effects. Because of the restricted geometric arrangement of the three donor atoms of the chelating ligand, the bond strength of each donor atom and the geometry of the complex will differ with increasing metal size. In the row from manganese to nickel only a small variation in the C═N wavelength (∼1588 cm^{-1}) was detected. Only complex **22b**

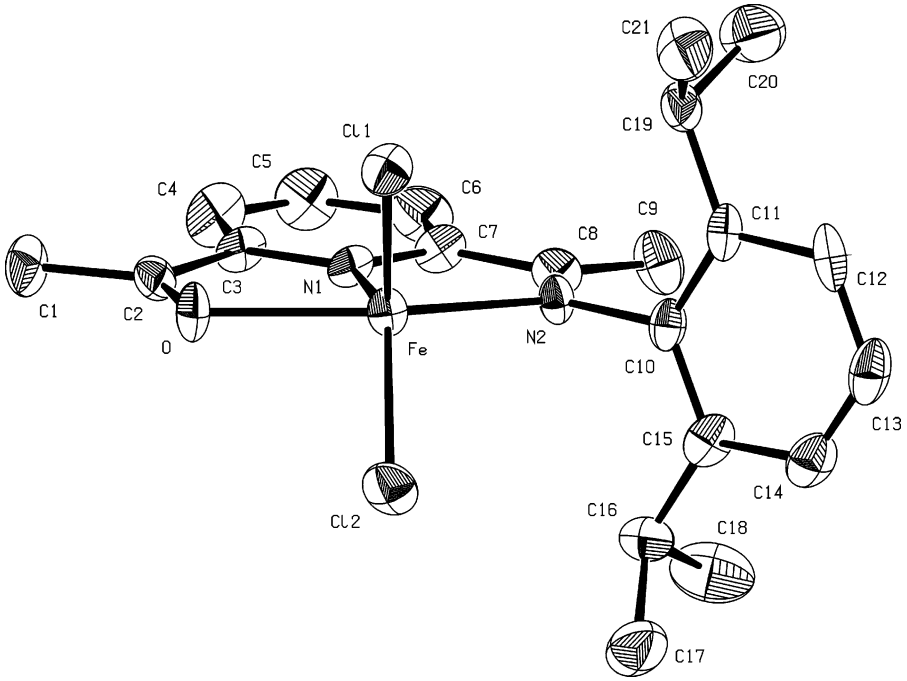

Figure 3. ORTEP style plot of complex **18** in the solid state. Thermal ellipsoids are drawn at the 50% probability level. Hydrogen atoms are omitted for clarity. Selected bond lengths (Å) and bond angles (deg) are given in Table 2.

Table 2. Selected Bond Distances (Å) and Angles (deg) for Complexes 15, 18·CH_2Cl_2, 21·CH_2Cl_2, and 22b

	15 (M = Fe, X = Cl)	**18**·CH_2Cl_2 (M = Fe, X = Cl)	**21**·CH_2Cl_2 (M = Co, X = Cl)	**22b** (M = Ni, X = Br)
M−N1	2.097(1)	2.102(5)	2.042(1)	1.981(2)
M−N2	2.195(1)	2.191(6)	2.161(1)	2.087(2)
M−N3	2.182(1)			
M−O		2.243(6)	2.327(1)	2.334(2)
M−X1	2.3224(6)	2.285(2)	2.2505(5)	2.4009(4)
M−X2	2.2732(5)	2.274(2)	2.2381(5)	2.3403(4)
C6/C8−N2	1.287(2)	1.307(9)	1.283(2)	1.278(3)
C2−O		1.224(10)	1.221(2)	1.213(4)
C8−N3	1.290(2)			
X1−M−X2	116.68(2)	107.95(8)	111.31(2)	117.76(2)
N1−M−N2	73.29(5)	73.8(2)	77.06(5)	78.69(8)
N1−M−O		71.7(2)	72.63(5)	73.45(8)
N1−M−N3	73.21(5)			
N2−M−O		145.1(2)	149.29(5)	148.56(8)
N2−M−N3	144.06(5)			
N1−M−X1	99.38(4)	119.5(2)	117.58(4)	94.47(6)
N2−M−X1	100.28(4)	106.5(2)	107.13(4)	104.42(6)
N1−M−X2	143.94(4)	131.1(2)	128.30(4)	146.12(6)
N2−M−X2	99.29(4)	105.0(2)	104.21(3)	101.33(6)
O−M−X1		94.8(2)	91.37(3)	92.15(5)
N3−M−X1	97.63(4)			
O−M−X2		93.9(2)	90.95(3)	93.95(5)
N3−M−X2	100.07(4)			

shows, at 1591 cm^{-1}, a slightly increased wavenumber, in accord with a higher number of electrons for the bromo substituent (lower electronegativity of bromine) and, for this reason, a lower Lewis acidity of the nickel(II) system. For the nickel complexes **23** and **24** the same results were obtained in the IR spectra.

Slow cooling of saturated dichloromethane (DCM) solutions of **18** and **21** deposited single crystals of purple and green crystals, respectively, which were suitable for X-ray diffraction. Red X-ray-quality crystals of complex **22b** were obtained by slow diffusion of *n*-pentane into a saturated DCM solution. Figure 3 illustrates the molecular structure of **18**, and Table 2 summarizes the selected bond distances and angles of complexes **18**, **21**, and **22b**. The structures of **21** and **22b** are similar to the structure of **18** and are depicted in the Supporting Information. Details of the data collection and refinement of the analysis are summarized in Table 3.

The square-pyramidal structure of **18** is reminiscent of certain five-coordinate iron(II) and cobalt(II) NNN derivatives reported by several research groups.[10,12,21,24] For complex **18** the basal plane consists of the two nitrogens and the oxygen atoms from the ligand and one equatorial chloride, with the remaining chloride (C11) occupying the apical position. In this geometry, the iron atom is raised 0.64 Å above the basal plane. In a comparison of complex **18** with **21**, a significant decrease in the metal−nitrogen bond length and also a significant decrease in the metal−chloro bond length were obtained. In contrast, the metal−oxygen bond length is increased from 2.243(6) Å (**18**) to 2.327(1) Å (**21**) (Table 2). The C(2)−O bond length is in both complexes equal within the esd's, in contrast to the C(8)−N(2) bond length (1.307(9) Å for **18**; 1.283(2) Å for **21**). In comparison to the case for the [bis(imino)pyridine]iron(II) complexes **12** and **15**, the two metal−chloro bond distances in complexes **18** and **21** vary only slightly (2.285(2) and 2.274(2) Å for **18**; 2.2505(5) and 2.2381(5) Å for **21**), in contrast to 2.266(2) and 2.311(2) Å for **12**[7a] and 2.2732(5) and 2.3224(6) Å for **15**. Complex **22b** has, as does complex **15**, a regular square-pyramidal structure.[38]

Polymerization. It is now well established that [bis(imino)-pyridine]iron(II) complexes can be activated by MAO and MMAO for the polymerization of ethene.[7−10] In the following discussion, a variety of different reaction temperatures and different cocatalyst/catalyst ratios are investigated for five bis-(imino)pyridine catalysts.

After activation with MMAO, complex **15** showed only very little activity in the polymerization of ethene or propene. At a temperature of 0 °C, insufficient activities of around 1400 kg of PE ((mol of Fe) h bar)$^{-1}$ were obtained for polymerization of ethene; when the temperature was increased to 40 °C, no polymerization was noted. Polymerization or oligomerization of propene was not successful with this catalyst

(38) Addison, A. W.; Rao, T. N.; Reedijk, J.; van Rijn, J.; Verschorr, G. C. *J. Chem. Soc., Dalton Trans.* **1984**, 1349.

Table 3. Crystallographic Data for Complexes 15, 18·CH_2Cl_2, 21·CH_2Cl_2, and 22b

	15	**18**·CH_2Cl_2	**21**·CH_2Cl_2	**22b**
formula	$C_{33}H_{27}Cl_2FeN_3$	$C_{22}H_{28}Cl_4FeN_2O$	$C_{22}H_{28}Cl_4CoN_2O$	$C_{21}H_{26}Br_2N_2NiO$
fw	592.33	534.11	537.19	540.93
color/habit	blue/plate	purple/needle	green/needle	red/fragment
cryst dimens (mm^3)	0.04 × 0.18 × 0.41	0.03 × 0.08 × 0.64	0.20 × 0.20 × 1.01	0.10 × 0.13 × 0.51
cryst syst	monoclinic	monoclinic	monoclinic	monoclinic
space group	$P2_1/n$ (No. 14)	$P2_1/c$ (No. 14)	$P2_1/c$ (No. 14)	Cc (No. 9)
a, Å	12.6461(3)	8.9356(8)	8.8222(1)	10.4153(2)
b, Å	16.1220(2)	15.1674(11)	15.2586(2)	16.0983(4)
c, Å	15.8418(3)	19.541(2)	19.5824(2)	13.4869(2)
β, deg	104.136(1)	101.885(11)	101.004(1)	92.393(1)
V, $Å^3$	3132.0(1)	2591.6(4)	2587.61(5)	2259.36(8)
Z	4	4	4	4
T, K	143	173	153	153
D_{calcd}, g cm^{-3}	1.256	1.369	1.379	1.590
μ, mm^{-1}	0.677	1.010	1.092	4.408
F(000)	1224	1104	1108	1088
θ range, deg	1.83−26.20	2.81−25.60	1.70−25.36	2.33−25.38
index ranges (h, k, l)	±15, ±20, ±19	−7 to +8, −17 to +14, ±23	±10, ±18, ±23	±12, ±19, ±16
no. of rflns collected	12 033	4300	9292	8080
no. of indep rflns/R_{int}	6247/0.020	2234/0.103	4744/0.010	4148/0.027
no. of obsd rflns ($I > 2\sigma(I)$)	5303	1450	4450	4028
no. of data/restraints/params	6247/0/460	2234/0 /271	4744/0 /383	4148/2 /348
R1/wR2 ($I > 2\sigma(I)$)[a]	0.0320/0.0712	0.0528/0.1295	0.0246/0.0591	0.0191/0.0434
R1/wR2 (all data)[a]	0.0401/0.0738	0.0870/0.1551	0.0268/0.0601	0.0202/0.0439
GOF (on F^2)[a]	1.027	0.953	1.042	1.042
largest diff peak/hole (e $Å^{-3}$)	+0.28/−0.41	+0.35/−0.45	+0.65/−0.48	+0.29/−0.23

[a] $R1 = \sum(||F_o| - |F_c||)/\sum|F_o|$; $wR2 = \{\sum[w(F_o^2 - F_c^2)^2]/\sum[w(F_o^2)^2]\}^{1/2}$; $GOF = \{\sum[w(F_o^2 - F_c^2)^2]/(n - p)\}^{1/2}$.

Table 4. Ethene and Propene Polymerization Activity of the Symmetrical [Bis(imino)pyridine]iron(II) Complex 13 after Activation with MMAO[a]

		activity[b]					
monomer	T (°C)	after 5 min	after 45 min	av	M_w[c]	M_n[c]	M_w/M_n[c]
ethene	0	79.8	15.4	21.2	1170	390	3.00
	20	99.7	29.7	40.9	1130	370	3.05
	40	93.2	3.57	18.1	930	300	3.10
	60	31.8	1.54	7.04	790	240	3.29
	80	8.52		2.12	670	200	3.35
propene	0	3.15	0.42	1.11	550	270	2.04
	20	2.02	0.22	0.82	400	200	2.00
	40	1.12	0.20	0.38	330	160	2.06
	60	–	–	–	–	–	–
	80	–	–	–	–	–	–

[a] Reaction conditions: 2 bar of alkene pressure, toluene as solvent, cocatalyst MMAO (Al:Fe = 1000); reaction time 1 h. [b] In units of 10^3 kg of PE/PP ((mol of Fe) h bar)$^{-1}$. [c] Determined by GPC.

under any conditions. It is tempting to attribute the low activity of complex **15** to the distorted catalyst geometry introduced by the sterically bulky biphenyl groups.

In contrast, complex **13** shows, after activation with MMAO, high activities of 10^4 kg of PE ((mol of Fe) h bar)$^{-1}$ for the polymerization of ethene, but the activity for the oligomerization of propene is much lower (see Table 4). We also found a temperature dependency for the polymerization of ethene. In contrast to the case for all other catalysts, the highest activity was obtained not at 0 °C but at 20 °C. The catalyst lifetime under the chosen reaction conditions has a large influence on the average polymerization activity. For this reason, at high reaction temperatures high starting activities and high maximum activities were observed; however, the average activities decreased rapidly at high temperatures. At 80 °C complete deactivation of the catalyst occurred after a short time (20 min). For all reactions no polymer was obtained, only oligomers with an average molecular weight of M_w = 700−1100. According to analytical GC-MS, short α-olefins such as 1-hexene and 1-octene were also obtained (Table 4). The polydispersity (M_w/M_n) for the formed oligomers was found to be 3, resulting from higher α-olefins being formed simultaneously with short-chain α-olefins. The two different groups of α-olefins presumably result from the large steric bulk of the N-aryl groups.

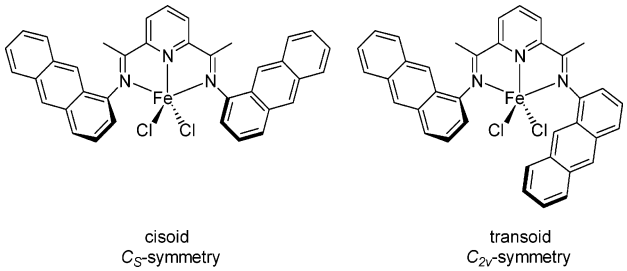

Figure 4. Possible conformations of complex **13**.

At higher temperatures the average activity for polymerization decreased and lower molecular weights of the products were observed, along with a concomitant decrease in selectivity and higher polydispersity.

Complex **13** can be found in two different conformations (with a C_s or a C_{2v} symmetry) (Figure 4). We propose for the poly- and oligomerization of propene a mechanism analogous to the polymerization of propene with activated *ansa*-metallocene complexes; thus, the two different conformers should yield a variety of poly- and oligopropylenes. In accordance with the well-known, related *ansa*-metallocene complexes, a conversion of the active center should occur during the chain-growing process, and the C_s-symmetric *cisoid* form should give predominantly atactic poly- or oligopropylene such as the symmetric *meso* form of *ansa*-bis(indenyl)metallocene derivatives.[39] According to this, the C_{2v}-symmetric *transoid* form should give isotactic poly- or oligopropylene, corresponding to the *rac* form of *ansa*-bis(indenyl)metallocene derivatives. Because of the hindered rotation flexibility of the N-aryl ring around the N−C_{aryl} bond, it should be possible at low temperatures to form either atactic or isotactic polymers.

(39) Wang, B. *Coord. Chem. Rev.* **2006**, *250*, 242 and references therein.

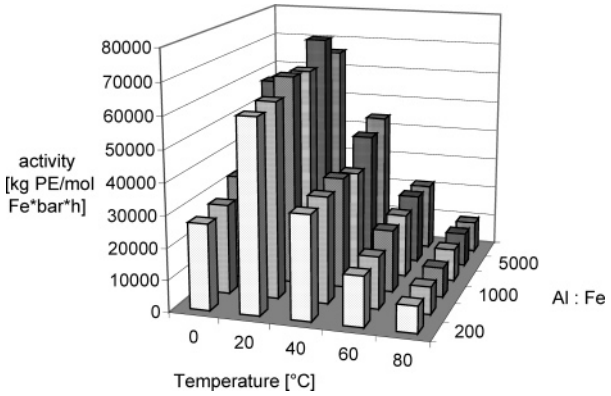

Figure 5. Ethene polymerization activity after activation of catalyst **14** with MMAO, dependent on the reaction temperature and cocatalyst/catalyst ratio.

During this work we were unable to obtain high isotactic oligomers with catalyst **13**. Only an enrichment of isotactic oligomer products was obtained, which can be explained by steric induction of the catalyst geometry, while no separation of the two catalyst modifications was successful during preparation (Figure 4). The formation of the *transoid* form should be favored during the preparation; for this reason an enrichment of isotactic oligomers was expected.

Also for complex **14** two conformers are possible, analogous to complex **13**. In spite of the C_s and C_{2v} symmetries of the catalyst, we were unable to obtain isotactic oligopropylene under any conditions. The {2,6-bis[((2-isopropylphenyl)imino)ethyl]-pyridine}iron complex **14** provides, with regard to propene polymerization, only a low polymerization activity of approximately 200 kg of PP ((mol of Fe) h bar)$^{-1}$, yielding atactic oligomers with a molecular weight of 300 and a polydispersity of 2.2.

In contrast, for ethene polymerization much higher activities were obtained, up to 73 $\times$ 10^3 kg of PE ((mol of Fe) h bar)$^{-1}$, but still polymers of lower molecular weight compared to those for complex **12** were obtained. This can be explained by the decreased steric hindrance imparted by the chelating ligand, where one ortho substituent at the N-aryl ring is missing compared to **12**. These aryl rings are less fixed orthogonal to the Fe$-$N$_3$ plane, and it follows that less blockage at the axial position of the catalyst increases the rate of the chain-transfer reaction and the formation of low-molecular-weight products. Catalyst **14** seems relatively insensitive toward changes in cocatalyst/catalyst ratio, as shown in Figure 5. In contrast, the polymerization activity is highly temperature dependent. The starting activity for catalyst **14** is relatively static at different temperatures up to 60 °C (see the Supporting Information), but the catalyst is deactivated more quickly with increasing temperatures. For this reason the average activity is calculated for all catalytic experiments after a reaction time of 60 min (Figure 5). The best results were obtained at a temperature of 20 °C. An increase or decrease of the reaction temperature resulted in severe suppression of catalytic activities. For example, an increase to 40 °C depressed the average activity to 60% of that obtained at 20 °C; further increases to 60 and 80 °C decreased the activity to 30% and 15%, respectively. The main reason for the rapid decrease in activity at high temperatures is the fast deactivation of the catalyst. At low temperatures (0 and 20 °C) the catalyst is still active after hours, while the catalytic activity at 60 °C stops after 40 min and that at 80 °C already after 30 min.

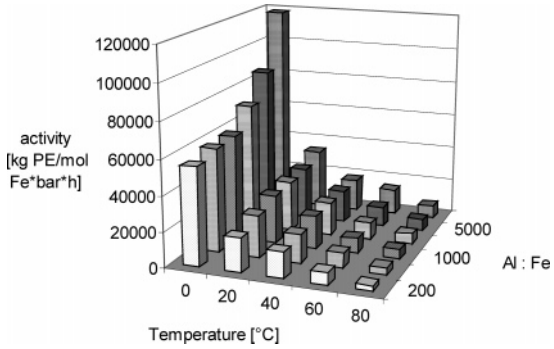

Figure 6. Ethene polymerization activity after activation of catalyst **17** with MMAO, dependent on the reaction temperature and cocatalyst/catalyst ratio.

We found with catalyst **14** a bimodal molecular weight distribution for all polymerization experiments. The polydispersity of the high-molecular-weight product decreases by changing the reaction temperature from 0 to 40 °C but increases if the temperature is changed to 60 or 80 °C. In contrast, such a tendency was not observed for the low-molecular-weight fraction; when the temperature was increased, a decrease in polydispersity was obtained (Supporting Information).

The polymerization properties and polymers of symmetric [bis(imino)pyridine]iron(II) chlorides have been well characterized in the literature;[7a,9,40] in this work catalyst **14** shows high-molecular-weight products and varying quantities of oligomers in the product spectra, whereas complex **12** forms nearly exclusively high-molecular-weight polymers.[7,10,30] For this reason it is of interest to use complex **17**, which could be thought of as a hybrid of complexes **12** and **14**, in polymerization reactions.

Similarly to the symmetric [bis(imino)pyridine]iron(II) complexes (**12**, **14**) an increase of the cocatalyst/catalyst ratio had only an insignificant effect on the polymerization activity of **17**; only for very high Al/Fe ratios (>5000) was there an increase in activity at low temperatures (10 °C). This catalyst also shows a high-temperature dependence for the polymerization activity; the best results were obtained at 0 °C (approximately 1 $\times$ 10^5 kg of PE ((mol of Fe) h bar)$^{-1}$). The activity maximum at this lower temperature is in agreement with the increase in steric bulk for the increasing number of isopropyl groups, in comparison with complex **14**. We were able to show for the hybrid complex **17** that an optimum temperature (0 °C) for catalysis should be chosen, which is between the optimal temperatures for complexes **12** (below 0 °C) and **14** (20 °C). If the temperature is increased to 20 °C, only 20% of the maximum activity at 0 °C was obtained. A further increase in temperature (up to 80 °C) gives only activities of around 5 $\times$ 10^3 kg of PE ((mol of Fe) h bar)$^{-1}$. For complex **17**, as for all previously discussed complexes (**12**$-$**14**), a very fast deactivation was recognized at high temperatures (Figure 6).

At low temperatures the produced polymers show only a small bimodality in the molecular weight distribution. Increasing the temperature to 20 °C results in a monomodal molecular weight distribution with polydispersities of up to 10. An increase in yield for the high-molecular-weight fraction was detected by the introduction of a third isopropyl group, such as for the unsymmetrical catalyst **17**. This introduction at the ortho position of the N-aryl ring results in a constant ethene polymerization

(40) (a) Britovsek, G. J. P.; Dorer, B. A.; Gibson, V.; Kimberley, B. S.; Solan, G. A. WO 9912981, 1997. (b) Small, B. L.; Brookhart, M. *Polym. Prepr.* (*Am. Chem. Soc., Div. Polym. Chem.*) **1998**, *39*, 213.

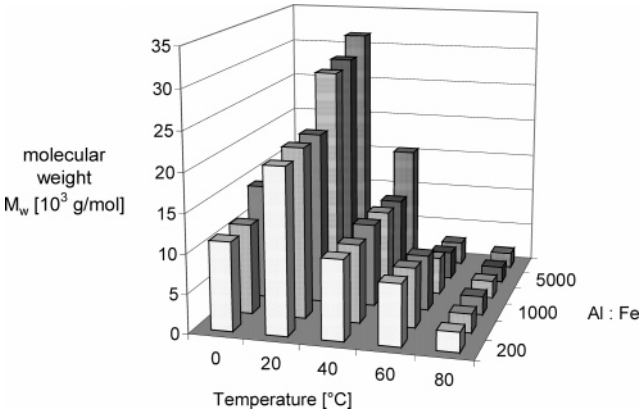

Figure 7. Molecular weight of the produced polymers obtained from ethene polymerization using catalyst **17**, dependent on the polymerization temperature and cocatalyst/catalyst ratio.

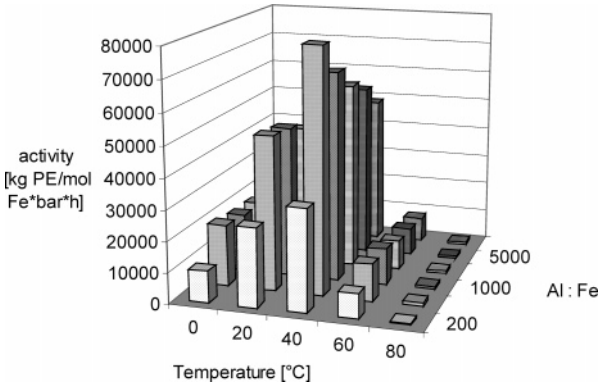

Figure 8. Ethene polymerization activity after activation of catalyst **16** with MMAO, dependent on the reaction temperature and cocatalyst/catalyst ratio.

activity. Because of the additional sterically bulky groups above or below the Fe−N_3 plane, the shielding of the axial positions at the N-aryl rings is optimized by an orthogonal fixation to the Fe−N_3 plane, yielding polymers with a high molecular weight of approximately 6×10^5 and small quantities of a low-molecular-weight fraction, with weights between 1×10^3 and 3×10^4; low-molecular-weight oligomers were not detected. The molecular weight for the high-molecular-weight polymers is still lower than those for the polymers obtained with catalyst **12**, where the axial positions are shielded by four isopropyl groups.

Changing the cocatalyst/catalyst ratio results only in small changes in the distribution; for an Al/Fe ratio of 1000, 4% of high-molecular-weight products was obtained, whereas at an Al/Fe ratio of 200 only 8% of high-molecular-weight products was recognized. As for the complexes above, the polymer distribution for catalyst **17** is highly sensitive toward changes in polymerization temperature. For this reason the highest molecular weights for polymers were obtained at 20 °C with an Al/Fe ratio of 10 000 (Figure 7).

The tendency to obtain high molecular weights with a high Al/Fe ratio is inverted at high temperatures. According to this behavior, it is necessary to use small Al/Fe ratios when using conditions above 40 °C. In this case no dependence of the molecular weight on the Al/Fe ratio could be determined (Figure 7).

The results of these experiments support the notion that complex **17** acts as a hybrid of the two symmetric complexes **12** and **14**. The polymerization activities are nearly the same for all of these catalysts; the catalytic properties of complex **17** lie between the data observed for the two symmetric complexes (**12**, **14**), as expected. With complex **17** we were unable to obtain molecular weights as high as those for complex **12**, but they are much higher than these obtained from catalyst **14**, which produces mainly low-molecular-weight products.

A comparison of the two symmetric catalysts **13** and **14** show that with the {2,6-bis[((isopropylphenyl)imino)ethyl]pyridine}-iron(II) complex **14** huge quantities of oligomers were obtained and also varying quantities of high-molecular-weight polymers. With catalyst **13** only oligomers were produced and never polymers. This is presumably because the 2,6-bis[(1-anthracenylimino)ethyl]pyridine ligand (**2**) has no bulky groups in the ortho position of the N-aryl rings, where an orthogonal orientation of the N-aryl rings to the Fe−N_3 plane is not restricted. Because of the lesser degree of hindrance at the axial position the chain transformation reaction is more favored, which results in low-molecular-weight polymers or oligomers.

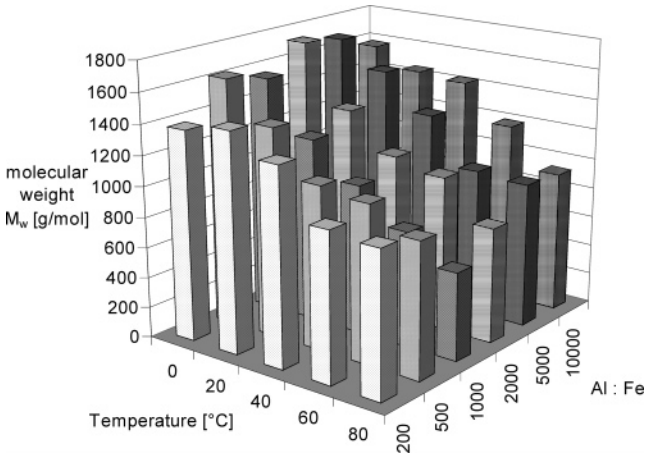

Figure 9. Molecular weight of the produced polymers obtained from ethene polymerization using catalyst **16**, dependent on the polymerization temperature and cocatalyst/catalyst ratio.

At this point, our interests now lay in the level of activity and the type of polymers that are obtained by using two isopropyl groups in positions ortho to an N-aryl ring and introducing on the other side one anthracenyl substituent; thus, we prepared complex **16**.

The polymerization activity of the unsymmetrical catalyst **16** was found to be equivalent to the symmetric catalysts **13** and **14**, but its activity maximum lay not at 0 or 20 °C but at a temperature of 40 °C, with activities of up to 8×10^4 kg of PE ((mol of Fe) h bar)$^{-1}$. When the temperature was either decreased or increased, a decrease in activity was obtained (Figure 8). The dependence of activity upon the cocatalyst/catalyst ratio is similar to that of the above catalysts and only plays a minor role in our experiments. The molecular weights of the formed products were slightly higher for catalyst **16** than for the symmetric catalyst **13**.

Analogous to the case for complex **13**, we could under no conditions obtain high-molecular-weight polymers with catalyst **16**; only oligomers with a molecular weight of 300−600 were produced. A slight cocatalyst/catalyst dependency was recognized for the produced polymers, as was true for all [bis(iminoethyl)pyridine]iron(II) complexes (**12**−**14**). The temperature dependence of the produced polymers is much less significant than for all previously discussed complexes (Figure 9). The highest molecular weights are obtained at the lowest temperature (0 °C). All experiments showed a polydispersity of approximately 3.

Table 5. Comparison of the Polymerization Activities and the Molecular Weight of the Produced Polymers Using Complexes 12−14, 16, and 17

complex	av polymerization activity[a]	mol wt	
		main product	minor product
12	10^3-10^5	10^5	10^3-10^4
17	10^3-10^5	10^4	10^5-10^6
14	10^3-10^5	10^2-10^3 ($T < 40$ °C)	10^4 ($T < 40$ °C)
		10^4-10^5 ($T > 40$ °C)	10^2-10^3 ($T > 40$ °C)
16	10^3-10^5	10^3	
13	10^3-10^5	10^2-10^3	

[a] Dependent on the reaction temperature; in units of kg of PE ((mol of Fe) h bar)$^{-1}$.

For propene polymerization only small activity was noted for complex **16**, in comparison to the results for the ethene polymerization. The average activity at 0 °C was 1500 kg of PP ((mol of Fe) h bar)$^{-1}$, which decreases rapidly at higher temperatures (60 °C). The oligomers obtained by reaction at 0 °C have a molecular weight of around 200; thus, in this case the temperature has only a very small influence on the molecular weight.

Conclusion

We were able to show a systematic dependence of the molecular weights of the polymers on the steric bulk of the substituents coordinated at the ortho position of the N-aryl groups. Using {2,6-bis[1-((2,6-diisopropylphenyl)imino)ethyl]-pyridine}iron(II) chloride (**12**), high-molecular-weight polyethylene was obtained;[7,10,30] however, if one isopropyl group is removed, such as in complex **17**, at low temperatures small quantities of high-molecular-weight polyethylene (6×10^5) were formed. The main product has a molecular weight of 10^4. If two isopropyl groups are removed, such as for the symmetric complex **14**, the molecular weight of the produced polymer is even lower than that of complex **12**. With complex **14** polymers of molecular weight 10^4-10^5, and large quantities of low-molecular-weight oligomers ($M_w = 10^2-10^3$) were obtained. These observations correlate very well with the steric hindrance of the ortho substituents of the N-aryl rings and results from the blockage of the axial position. With this blockage of the axial positions chain transfer reactions are disfavored, which results in higher molecular weight polymers. Similar trends were obtained for the reaction temperature dependence. For the less sterically bulky complex **14**, the best results were obtained at 20 °C; when the steric hindrance of the complex was increased, as in complex **17**, the maximum activity was obtained at lower temperatures (0 °C).

For polymerization activities of the homologous row of complexes nearly equal or identical values were obtained; changes at the ortho substituents result only in an increase or decrease in molecular weight of the product polymers, not in the activity of the catalyst (Table 5).

Similar trends were obtained by replacing the (2,6-diisopropylphenyl)imino group of the {2,6-bis[1-((2,6-diisopropylphenyl)-imino)ethyl]pyridine}iron(II) chloride complex **12** by an anthracenylimino group. The steric bulk of the resulting complex **16** is decreased dramatically, such that only oligomers with molecular weights of 500−1000 were observed. When both (2,6-diisopropylphenyl)imino groups were substituted by anthracenyl groups (as in complex **13**), even smaller molecular weight oligomers were obtained in insignificant concentrations. These observations correlate very well with the decreased steric hindrance of the ortho substituents of the N-aryl rings, where no stabilization of the orthogonal FeN_3 plane is favored, and low-molecular-weight oligomers occur by chain transfer reaction (Table 5).

Experimental Section

General Considerations. All experiments were carried out under an atmosphere of dry, purified nitrogen or argon using glovebox or standard Schlenk techniques. All solvents were dried and deoxygenated and kept under argon and molecular sieves (4 Å). NMR spectra were recorded on JEOL JNM GX-400 and Bruker DPX-400 instruments. The solvent signals were used for internal calibration. All spectra were obtained at room temperature unless otherwise stated. The infrared spectra of the homogeneous compounds were recorded on a Perkin-Elmer FT-IR 1650 instrument as KBr pellets. The supported precatalyst samples were prepared under an inert atmosphere as self-supporting pellets and analyzed using NaCl windows. Elemental analyses were carried out by the Microanalytical Laboratory at the TU München. Mass spectra were performed at the TU München Mass Spectrometry Laboratory on a Finnigan MAT 90 spectrometer using the CI or FAB technique. Melting points were measured with a Büchi melting point apparatus system (Dr. Tottoli). Polymer samples were dissolved in a mixture of d_3-1,2,4-trichlorobenzene and $C_2D_2Cl_4$ and analyzed via NMR spectroscopy at a temperature of 120 °C. The obtained polymers were analyzed using a combination of a Waters 150 CV high-temperature GPC at 135 °C with 1,2,4-trichlorobenzene as solvent and a modified Whyatt Minidawn light-scattering instrument. The calibration was performed with polystyrene standards and conversion into PE and PP calibration curves using Mark−Houwink parameters. Modified methylaluminoxane (Witco, 10% in *n*-heptane) was used as cocatalyst. Ethene (AGA Gas GmbH, grade 3.5) and propene (Linde AG, grade 2.8) were purified by passing them through two purification columns containing activated BTS catalyst and molecular sieves (4 Å) before feeding the reactor. The reactor pressure (2 bar ± 0.02) was maintained constant throughout the polymerization run by a press flow gas controller (Büchi bpc 1202). 2,6-Bis{1-[(2,6-diisopropylphenyl)imino]ethyl}pyridine (**1**),[10,41] 2,6-bis[1-(anthracenylimino)ethyl]pyridine (**2**),[42,43] 2,6-bis{1-[(2-isopropylphenyl)imino]ethyl}pyridine (**3**),[8,30,32,44] 2,6-bis[1-(1-biphenylimino)ethyl]pyridine (**4**),[42,45] 2-acetyl-6-{1-[(2,6-diisopropylphenyl)-imino]ethyl}pyridine (**5**),[46,47] 2-acetyl-6-{1-[(2,6-dimethylphenyl)-imino]ethyl}pyridine (**7**),[36,47,48] 2-{1-[(2-isopropylphenyl)imino]ethyl}-6-{1-[(2,6-diisopropylphenyl)imino]ethyl}pyridine (**9**),[44] {2,6-bis-[1-((2,6-diisopropylphenyl)imino)ethyl]pyridine}iron(II) chloride (**12**),[7a,10,30a] {2,6-bis[1-(anthracenylimino)ethyl]pyridine}iron(II) chloride (**13**),[49] {2,6-bis[1-((2-isopropylphenyl)imino)ethyl]pyridine}-iron(II) chloride (**14**),[30,50] {2-[1-((2-isopropylphenyl)imino)ethyl]-6-[1-((2,6-diisopropylphenyl)imino)ethyl]pyridine}iron(II) chloride (**17**),[16] {2-acetyl-6-[1-((2,6-diisopropylphenyl)imino)ethyl]pyridine}-iron(II) chloride (**18**),[34] and {2-acetyl-6-[1-((2,6-diisopropylphenyl)-imino)ethyl]pyridine}chromium(II) chloride (**19**)[36] were prepared according to published methods.

(41) Brookhart, M. S.; Small, B. L. WO 9830612 A1, 1998.
(42) Schmidt, R.; Hammon, U.; Welch, M. B.; Alt, H. G.; Hauger, B. E.; Knudsen, R. D. U.S. Patent 6458905 B1, 2002.
(43) Benvenuti, F.; Francois, P. Eur. Patent EP 1260515 A1, 2002.
(44) Ma, Z.; Sun, W.-H.; Li, Z.-L.; Shao, C.-X.; Hu, Y.-L. *Chin. J. Polym. Sci.* **2002**, *20*, 205.
(45) Bennett, A. M. A. WO 9951550 A1, 1999.
(46) Gibson, V. C.; Kimberley, B. S.; Solan, G. A. WO 2000020427 A1, 2000.
(47) Bianchini, C.; Mantovani, G.; Meli, A.; Migliacci, F.; Zanobini, F.; Laschi, F.; Sommazzi, A. *Eur. J. Inorg. Chem.* **2003**, 1620.
(48) Mestroni, G.; Bianchini, C.; Sommazzi, A.; Milani, B.; Mantovani, G.; Masi, F.; Meli, A.; Santi, R. WO 2002010133 A1, 2002.
(49) Benvenuti, F.; Francois, P., Razavi, A.; Marin, V.; Lopez, M. U.S. Patent 2005090631 A1, 2005.
(50) Gibson, V. C. WO 9830612, 1998; WO 9902472 A1, 1999.

2,6-Bis[1-(anthracenylimino)ethyl]pyridine (2). This compound was prepared according to the method given in the literature.[42,43] Yield: 77%. Mp: 220 °C dec. Anal. Calcd for $C_{37}H_{27}N_3$ (513.63): C, 86.52; H, 5.30; N, 8.18. Found: C, 86.18; H, 5.47; N, 7.86. ^{1}H NMR ($CDCl_3$): δ 2.47 (s, 6H, $CH_3C{=}N$), 6.82 (d, 2H, $^3J_{HH} = 6.7$ Hz), 7.42−7.51 (m, 6H), 7.82 (d, 2H, $^3J_{HH} = 8.2$ Hz), 7.97 (d, 2H, $^3J_{HH} = 8.2$ Hz), 8.01 (d, 2H, $^3J_{HH} = 8.2$ Hz), 8.09 (t, 1H, $^3J_{HH} = 7.5$ Hz), 8.39 (s, 2H), 8.48 (s, 2H), 8.73 (d, 2H, $^3J_{HH} = 7.5$ Hz, py). $^{13}C\{^1H\}$ NMR ($CDCl_3$): δ 16.5 (N=C*Me*), 111.6, 122.3, 122.8, 124.0, 125.2 (C_{quat}), 125.3, 125.3, 125.6, 126.3, 128.0, 128.6, 131.4 (C_{quat}), 131.9 (C_{quat}), 132.3 (C_{quat}), 137.2, 147.5 (C_{quat}), 155.5 (C_{quat}), 168.5 (*C*=N). IR (KBr): ν 3045.8 m, 2923.1 m, 1633.0 s (2 C=N), 1566.7 m, 1556.6 m, 1536.0 m, 1453.4 m, 1360.0 m, 1311.4 m, 1240.3 m, 1193.7 m, 1119.8 m, 957.1 w, 875.2 s, 821.7 m, 803.2 m, 730.0 s, 471.1 m cm^{-1}. MS (CI): *m*/*z* 513.4 [M^+]; 498.3 [M^+ − Me]; 321.2 [$M^+ - NHC_{14}H_9$].

2,6-Bis[1-(1-biphenylimino)ethyl]pyridine (4). This compound was prepared according to the method given in the literature.[42,45] Yield 88%. Mp: 145 °C. Anal. Calcd for $C_{33}H_{27}N_3$ (465.59): C, 85.13; H, 5.85; N, 9.03. Found: C, 85.04; H, 5.81; N, 9.00. ^{1}H NMR ($CDCl_3$): δ 2.13 (s, 6H, *Me*C=N), 6.79 (d, 2H, $J_{HH} = 7.5$ Hz, aryl), 7.19 (t, 4H, $J_{HH} = 7.5$ Hz, aryl), 7.27 (t, 4H, $J_{HH} = 7.5$ Hz, aryl), 7.33 (dt, 2H, $J_{HH} = 8.0$ Hz, aryl), 7.40 (d, 6H, $J_{HH} = 8.0$ Hz, aryl), 7.75 (t, 1H, $J_{HH} = 7.7$ Hz, H_p py), 8.09 (d, 2H, $J_{HH} = 8.0$ Hz, H_m py). $^{13}C\{^1H\}$ NMR ($CDCl_3$): δ 17.1 (*Me*C=N), 119.8, 122.5, 124.4, 126.2 (C_{quat}), 126.9, 128.2, 129.5, 130.7, 132.1 (C_{quat}), 137.1, 140.2 (C_{quat}), 149.1 (C_{quat}), 155.4 (C_{quat}), 167.4 (*C*=N). IR (KBr): ν 3046.7 m, 1649.4 s, 1575.9 m, 1566.8 m, 1472.7 s, 1432.4 m, 1363.6 s, 1249.2 m, 1209.9 s, 1111.6 m, 1008.5 w, 825.3 m, 771.4 m, 741.5 s, 698.8 s, 645.8 w, 615.0 w, 500.3 w cm^{-1}. MS (CI): *m*/*z* 465.1 [M^+], 449.9 [M^+ − Me], 312.0 [$M^+ - C_6H_8^+$], 152.1 [$C_6H_8^+$].

2-Acetyl-6-{1-[(2-isopropylphenyl)imino]ethyl}pyridine (6). A 2.00 g portion (12.2 mmol) of 2,6-diacetylpyridine was dissolved in 50 mL of EtOH and reacted with 0.98 equiv (11.9 mmol, 1.65 mL) of 2-isopropylaniline, acetic acid (100%; 0.1 mL) and molecular sieves (4 Å). The reaction mixture was refluxed for 24 h, and afterward the solution was filtered and washed twice with 20 mL of EtOH. The yellow solution was stored at −30 °C overnight to precipitate the side product. The mother liquor was reduced to half of the original volume and stored at −30 °C to precipitate the second fraction. The second fraction was dried in vacuo to give the desired product as a yellow powder in 53% yield (6.3 mmol, 1.76 g). Mp: 76 °C. Anal. Calcd for $C_{18}H_{20}N_2O$ (280.36): C, 77.11; H, 7.19; N, 9.99. Found: C, 76.88; H, 7.02; N, 10.09. ^{1}H NMR ($CDCl_3$): δ 1.17 (d, 6H, $J_{HH} = 7.1$ Hz, C*H*Me_2), 2.37 (s, 3H, *Me*C=N), 2.77 (s, 3H, *Me*C=O), 2.93−3.00 (q, 1H, $J_{HH} = 7.0$ Hz, C*H*Me_2), 6.61 (d, 1H, $J_{HH} = 7.5$ Hz, aryl), 7.02 (t, 1H, $J_{HH} = 7.6$ Hz, aryl), 7.17 (t, 1H, $J_{HH} = 7.5$ Hz, aryl), 7.31 (d, 1H, $J_{HH} = 7.5$ Hz, aryl), 7.91 (t, 1H, $J_{HH} = 7.6$ Hz, H_p py), 8.10 (d, 1H, $J_{HH} = 7.4$ Hz, H_m py), 8.50 (d, 1H, $J_{HH} = 7.2$ Hz, H_m py). $^{13}C\{^1H\}$ NMR ($CDCl_3$): δ 16.2 (*Me*C=N), 22.8 (CH*Me*$_2$), 25.6 (*Me*C=O), 28.4 (*C*HMe_2), 118.2, 122.4, 124.2, 124.6, 125.7, 126.1, 137.2, 138.1 (C_{quat}), 148.4 (C_{quat}), 152.4 (C_{quat}), 155.9 (C_{quat}), 165.9 (*C*=N), 200.1 (*C*=O). IR (KBr): ν 3059.8 m, 2960.4 s, 2925.1 m, 2871.6 w, 1695.6 s, 1647.6 s, 1592.3 m, 1578.0 m, 1481.8 s, 1443.6 s, 1406.8 m, 1361.8 s, 1311.9 m, 1243.9 s, 1221.5 s, 1145.6 w, 1114.4 s, 1075.7 m, 1033.9 m, 994.1 m, 947.4 m, 821.8 s, 804.0 m, 768.0 m, 748.6 s, 724.6 m, 690.6 w, 646.4 w, 596.3 m, 494.2 w, 420.3 w cm^{-1}. MS (CI): *m*/*z* 280.2 (M^+), 265.1 (M^+ − Me). GC-MS: $R_t = 22.13$ min; *m*/*z* 280 [M^+], 265 [M^+ − Me], 250 [M^+ − Me], 160 [$M^+ - C_9H_{12}$], 144 [$M^+ - NC_8H_{10}$].

2-[1-(Anthracenylimino)ethyl]-6-{1-[(2,6-(diisopropylphenyl)-imino]ethyl}pyridine (8). A 0.37 g portion of 1-aminoanthracene (1.92 mmol, 0.98 equiv) was added to a stirred solution of **5** (0.63 g, 1.96 mmol) in toluene (40 mL). Molecular sieves (4 Å) and 10 mg of *p*-toluenesulfonic acid were used as drying agent and catalyst. After 5 days under reflux conditions the reaction suspension was filtered and the residue was washed with toluene. The reddish toluene solution was removed in vacuo, and the red-brown solid was washed twice with methanol (10 mL). The yellow product **8** was isolated by filtration and dried in vacuo. Yield: 1.25 g (62%). Mp: 180 °C dec. Anal. Calcd for $C_{35}H_{35}N_3$ (497.67): C, 84.47; H, 7.09; N, 8.44. Found: C, 83.93; H, 7.45; N, 8.06. ^{1}H NMR (−40 °C, toluene-d_8): δ 0.90 (s, 3H, CHMe_2, rotamer I), 0.99 (d, 3H, $^3J_{HH} = 8.0$ Hz, CHMe_2, rotamer I), 1.15 (br, 12H, CHMe_2, rotamer II), 1.23 (br, 6H, CHMe_2, rotamer I), 2.35 (s, 3H, *Me*C=N), 2.43 (s, 3H, *Me*C=N), 2.59 (m, 1H, C*H*Me_2, rotamer I), 2.85 (m, 1H, C*H*Me_2, rotamer I), 2.97 (m, 2H, C*H*Me_2, rotamer II), 6.15 (s, 1H, aryl), 6.37 (s, 1H, aryl), 7.18−7.23 (m, 5H, aryl), 7.40 (s, 1H, aryl), 7.51 (m, 1H, aryl), 7.71−7.76 (m, 2H, aryl), 8.06 (s, 1H, aryl), 8.21 (s, 1H, aryl), 8.42 (s, 1H, aryl), 8.58 (s, 1H, aryl). $^{13}C\{^1H\}$ NMR (CD_2Cl_2): δ 16.6 (N=C*Me*), 17.4 (N=C*Me*), 22.6 (CH*Me*), 22.9 (CH*Me*), 23.2 (CH*Me*), 23.4 (CH*Me*), 28.4 (*C*HMe), 28.6 (*C*HMe), 117.1, 119.5, 119.6, 120.2, 121.2, 123.2, 123.3, 123.8, 124.6, 125.0, 125.7, 126.1, 126.9, 128.2, 128.6, 131.5, 132.2, 132.5, 136.1, 136.2, 137.4, 137.5, 137.9, 139.6, 146.8, 147.0, 155.9 (aryl), 165.5 (*C*=N), 167.4 (*C*=N). IR (KBr): ν 3062.1 m, 2961.1 s, 2923.1 m, 2861.5 m, 1646.6 s, 1569.0 s, 1456.0 s, 1400.0 w, 1363.2 m, 1300.0 w, 1260.4 m, 1111.6 m, 1015.4 m, 814.3 s, 738.5 w, 668.4 m cm^{-1}. MS (CI): *m*/*z* 496.8 [M^+], 480.9 [M^+ − Me], 465.9 [M^+ − 2 Me].

2-{1-(2-Isopropylphenyl)imino]ethyl}-6-{1-[(2,6-diisopropyl-phenyl)imino]ethyl}pyridine (9). A 0.4 mL portion (2.80 mmol, 2 equiv) of 2-isopropylaniline was added to a stirred solution of **5** (0.45 g, 1.40 mmol) in toluene (30 mL). Molecular sieves (4 Å) and 10 mg of *p*-toluenesulfonic acid were used as drying agent and catalyst. After 24 h under reflux conditions the reaction suspension was filtered and the residue was washed with toluene. The toluene solution was removed by filtration, and the solid was washed twice with methanol (10 mL) and dried in vacuo. Yield: 350 mg (57%). Mp: 158 °C. Anal. Calcd for $C_{30}H_{37}N_3$ (439.64): C, 81.96; H, 8.48; N, 9.56. Found: C, 81.45; H, 8.64; N, 9.33. ^{1}H NMR ($CDCl_3$): δ 1.15 (d, 12H, $^3J_{HH} = 6.9$ Hz, CHMe_2), 1.19 (d, 6H, $^3J_{HH} = 6.8$ Hz, CHMe_2), 2.27 (s, 3H, N=C*Me*), 2.39 (s, 3H, N=C*Me*), 2.77 (sept., 2H, $^3J_{HH} = 6.9$ Hz, C*H*Me_2), 3.02 (sept, 1H, $^3J_{HH} = 6.8$ Hz, C*H*Me_2), 6.64 (d, 1H;$^3J_{HH} = 8.0$ Hz, aryl), 7.08−7.13 (m, 2H, aryl), 7.17−7.21 (m, 3H, aryl), 7.32 (d, 1H, $^3J_{HH} = 7.8$ Hz, aryl), 7.91 (t, 1H, $^3J_{HH} = 7.6$ Hz, H_p py), 8.40−8.55 (m, 2H, H_m py). $^{13}C\{^1H\}$ NMR ($CDCl_3$): δ 16.4 (N=C*Me*), 17.1 (N=C*Me*), 22.8 (CHMe_2), 22.9 (CHMe_2), 23.2 (CHMe_2), 28.3 (*C*HMe_2), 28.5 (*C*HMe_2), 118.4, 122.1, 122.3, 123.0, 123.6, 124.0, 125.7, 126.1, 135.8, 136.8, 138.1, 146.5, 148.7, 155.1, 155.6 (aryl), 166.5 (*C*=N), 166.9 (*C*=N). IR (KBr): ν 3065.5 m, 2959.7 s, 2925.1 m, 2866.2 m, 1637.6 s (C=N), 1594.5 m, 1567.6 m, 1480.1 m, 1455.1 m, 1381.7 m, 1364.2 s, 1222.9 m, 1191.8 m, 1122.6 m, 1075.9 w, 829.5 m, 777.6 m, 762.2 m, 750.8 m cm^{-1}. MS (CI): *m*/*z* 439 [M^+], 424 [M^+ − Me], 397 [$M^+ - C(Me)_2$], 382 [$M^+ - (C(Me)_2$ + Me)].

Styrol-Functionalized, 4-Vinylbenzyl-Functionalized 2,6-Bis-{1-[(2,6-diisopropylphenyl)imino]ethyl}pyridine (10). A 2.00 g (4.15 mmol) portion of compound **1** was dissolved in 70 mL of THF, and with vigorous stirring 1.03 equiv (4.27 mmol, 2.14 mL) of LDA was added to the reaction solution. After 14 h 1 equiv (4.15 mmol, 0.58 mL) of 4-vinylbenzyl chloride was added to the dark green solution. The combined reaction mixture was stirred for 5 days under reflux. Afterward, the solvent was evaporated, the reddish precipitate was extracted three times with 20 mL of *n*-pentane, and the extracts were filtered. The filtrate was dried in vacuo. The red solid was washed with ethanol and dried to give complex **10** in 40% yield (1.00 g). Anal. Calcd for $C_{42}H_{51}N_3$ (597.87): C, 84.37; H, 8.60; N, 7.03. Found: C, 83.96; H, 8.31; N, 6.59. MS (CI): *m*/*z* 597.4 [M^+], 582.4 [M^+ − Me], 554.4 [M^+ − (Me + vinyl)]. Two stereoisomers were obtained in a 3:1 ratio.

Main isomer: ^{1}H NMR ($CDCl_3$) δ 1.14−1.25 (m, 24H, HC*Me*$_2$), 2.31 (s, 3H, *Me*$_2$C═N), 2.74−2.84 (m, 6H, *HC*Me$_2$ & ^{1}C*H*$_2$), 2.96−3.01 (m, 2H, ^{2}C*H*$_2$), 5.14 (d, 1H, J_{HH} = 10.9 Hz, CH═C*H*$_2$), 5.62 (d, 1H, J_{HH} = 17.6 Hz, CH═C*H*$_2$), 6.57 (dd, 1H, J_{HH} = 17.5, 10.9 Hz, CH═C*H*$_2$), 6.95 (d, 2H, J_{HH} = 7.9 Hz, styrene), 7.08−7.12 (m, 2H, aryl), 7.17−7.19 (m, 4H, aryl), 7.21 (d, J_{HH} = 7.9 Hz, styrene), 7.96 (t, 1H, J_{HH} = 7.9 Hz, H_p py), 8.48 (pseudo-t, 2H, H_m py); ^{13}C{^{1}H} NMR ($CDCl_3$) δ 17.4 (*Me*C═N), 22.2 (CH*Me*$_2$), 22.9 (CH*Me*$_2$), 23.2 (CH*Me*$_2$), 23.6 (CH*Me*$_2$), 28.3 (*CH*Me$_2$), 28.4 (*CH*Me$_2$), 28.4 (*CH*Me$_2$), 32.5 (*C*2), 32.6 (C1), 113.2 (CH═*CH*$_2$), 122.2 (C_m py), 123.0 (aryl), 123.0 (aryl), 123.1 (C_m py), 123.6 (styrene), 126.3 (aryl), 126.6 (C_{quat}), 128.2 (styrene), 135.3 (C_{quat}), 135.5 (C_{quat}), 136.4 (*CH*═CH$_2$), 137.1 (C_p py), 141.3 (C_{quat}), 146.0 (C_{quat}), 146.5 (C_{quat}), 145.5 (C_{quat}), 155.3 (C_{quat}), 166.8 (*C*═N), 168.4 (*C*═N); IR (KBr) ν 3060.5 w, 2960.3 s, 2925.6 m, 2866.3 m, 1634.0 s, 1568.1 w, 1510.9 w, 1457.0 m, 1362.6 s, 1323.0 w, 1237.0 m, 1192.5 m, 1109.8 m, 988.0 w, 904.7 w, 825.8 m, 759.9 m, 690.9 w cm^{-1}.

{**2,6-Bis[1-(anthracenylimino)ethyl]pyridine**}**iron(II) Chloride (13)**. To a solution of 179 mg of $Fe^{II}Cl_2$·4H_2O (0.9 mmol) in 10 mL of *n*-BuOH was slowly added a solution of 500 mg of ligand **2** (0.97 mmol) in 20 mL of *n*-BuOH. The color changed rapidly to dark green. The suspension was heated for 30 min at 90 °C and cooled over a period of 14 h to room temperature. The solvent was removed in vacuo, and the dark green residue was washed with 10 mL of diethyl ether and 10 mL of *n*-pentane. Yield: 0.57 g (98%). Mp: 255 °C dec. Anal. Calcd for $C_{37}H_{27}N_3Cl_2Fe$ (640.38): C, 69.40; H, 4.25; N, 6.56. Found: C, 68.98; H, 4.51; N, 6.14. IR (KBr): ν 3049.9 s, 1618.5 s, 1584.1 s, 1593.5 m, 1455.4 m, 1426.6 m, 1371.2 s, 1311.6 m, 1267.3 s, 1208.0 m, 1132.3 w, 1030.9 w, 881.8 s, 810.2 m, 743.1 s, 732.2 s, 473.5 m cm^{-1}. MS (FAB): *m*/*z* 638.7 [M$^+$ − H], 603.7 [M$^+$ − ClH].

{**2,6-Bis[1-(1-biphenylimino)ethyl]pyridine**}**iron(II) Chloride (15)**. A 860 mg (1.85 mmol) portion of ligand **4** was added to 0.95 equiv (340 mg) of $FeCl_2$·4H_2O. After addition of 10 mL *n*-BuOH the suspension changed color to dark green. The suspension was stirred for 14 h at room temperature and was filtered afterward. The residue was washed twice with 10 mL of toluene to give 0.93 g (90%) of complex **15**. Suitable crystals were obtained by slow diffusion of diethyl ether into a concentrated DCM solution of complex **15**. Anal. Calcd for $C_{33}H_{27}N_3Cl_2Fe$ (592.34): C, 66.91; H, 4.59; N, 7.09. Found: C, 66.52; H, 4.82; N, 6.84. IR (KBr): ν 3053.8 m, 2961.5 m, 1621.6 m, 1589.7 m, 1475.9 m, 1431.7 m, 1374.1 m, 1262.2 s, 1176.6 vs, 1046.4 m, 877.8 s, 812.1 m, 782.6 m, 745.6 s, 704.2 s, 573.8 s, 537.9 m cm^{-1}. MS (FAB): *m*/*z* 592.8 [M$^+$], 557.6 [M$^+$ − Cl], 521.7 [M$^+$ − 2Cl], 465.9 [M$^+$ − (2Cl, Fe)].

{**2-[1-(Anthracenylimino)ethyl]-6-[1-((2,6-diisopropylphenyl)-imino)ethyl]pyridine**}**iron(II) Chloride (16)**. To a solution of 217 mg of $Fe^{II}Cl_2$·4H_2O (1.09 mmol) in 10 mL of *n*-BuOH was added 570 mg of ligand **8** (suspended in 20 mL of *n*-BuOH). The suspension was heated for 30 min at 90 °C, and afterward the dark green suspension was stirred overnight at room temperature. The solvent was removed in vacuo, and the green-bronze residue was washed with 10 mL of diethyl ether and 10 mL of *n*-pentane. Yield: 0.44 g (64%). Mp: 235 °C dec. Anal. Calcd for $C_{35}H_{35}N_3$-Cl_2Fe (624.42): C, 67.32; H, 5.65; N, 6.73. Found: C, 67.65; H, 5.18; N, 6.40. IR (KBr): ν 3046.2 m, 2953.8 m, 1618.0 w, 1584.5 m, 1540.0 w, 1456.0 w, 1369.3 m, 1311.9 w, 1260.3 m, 1205.3 w, 1100.0 w, 876.0 s, 808.3 s, 730.9 s, 470.5 m cm^{-1}. MS (FAB): *m*/*z* 623.8 [M$^+$], 608.8 [M$^+$ − Me], 588.1 [M$^+$ − Cl], 396.8 [M$^+$ − (Cl, $NHC_{14}H_9$)].

{**2-[1-((2-Isopropylphenyl)imino)ethyl]-6-[1-((2,6-diisopropyl-phenyl)imino)ethyl]pyridine**}**iron(II) Chloride (17)**. To a solution of 117 mg of $Fe^{II}Cl_2$·4H_2O (0.95 mmol) in 10 mL of THF was added 260 mg of ligand **9**. The color rapidly changed to dark blue. The suspension was stirred for 14 h at room temperature. The solvent was removed by filtration, and the precipitate was dried in vacuo. Yield: 0.30 g (92%). Mp: 230 °C dec. Anal. Calcd for $C_{30}H_{37}N_3Cl_2Fe$ (566.39): C, 63.62; H, 6.58; N, 7.42. Found: C, 63.45; H, 6.82; N, 7.12. IR (KBr): ν 3069.9 m, 2962.1 s, 2923.1 m, 2867.7 m, 1622.1 m, 1584.5 s, 1484.2 m, 1443.7 m, 1371.5 s, 1264.3 s, 1225.1 m, 1205.0 m, 1103.4 w, 1059.2 w, 1031.6 w, 813.3 m, 781.6 m, 753.7 m cm^{-1}. MS (FAB): *m*/*z* 565.2 [M$^+$], 530.4 [M$^+$ − Cl], 514.4 [M$^+$ − (Cl, Me)], 495.5 [M$^+$ − 2Cl].

Styrol-Functionalized [Bis(imino)pyridine]iron(II) Complex 11. To 200 mg of ligand **10** (0.34 mmol) dissolved in 15 mL of THF was added 0.98 equiv of $FeCl_2$·4H_2O (65 mg). The solution was stirred for 14 h and the product precipitated after the addition of 20 mL of *n*-pentane at −2 °C. After filtration and drying in vacuo complex **11** was obtained in 66% yield (157 mg). Mp: >250 °C. Anal. Calcd for $C_{42}H_{51}N_3Cl_2Fe$ (724.62): C, 69.62; H, 7.09; N, 5.80. Found: C, 69.12; H, 7.28; N, 5.65. IR (KBr): ν 3061.0 m, 2962.7 s, 2926.0 m, 2866.9 m, 1625.5 m, 1577.1 s, 1511.8 w, 1464.5 s, 1383.8 m, 1371.1 m, 1325.4 w, 1269.8 m, 1203.7 w, 1186.3 w, 1103.7 m, 1057.0 m, 988.7 w, 936.5 w, 823.4 w, 815.3 m, 797.9 m, 777.3 m, 715.3 w cm^{-1}. MS (FAB): *m*/*z* 723.8 [M$^+$], 688.7 [M$^+$ − Cl], 653.6 [M$^+$ − 2Cl], 597.9 [M$^+$ − $FeCl_2$].

{**2-Acetyl-6-[1-((2,6-diisopropylphenyl)imino)ethyl]pyridine**}-**manganese(II) Chloride (20)**. To 200 mg (0.62 mmol) of ligand **5** was added 0.98 equiv of $MnCl_2$·4H_2O (119 mg) in a Schlenk tube. After addition of 15 mL of THF a yellow suspension was formed, and after 15 min the solution became cloudy. The solution was stirred at 50 °C for 14 h to give a beige suspension. The residue was obtained by filtration and was washed twice with 10 mL of DCM. After drying in vacuo complex **20** was obtained in 67% (177 mg) yield. Anal. Calcd for $C_{21}H_{26}N_2Cl_2MnO$ (448.29): C, 56.26; H, 5.85; N, 6.25. Found: C, 56.97; H, 6.31; N, 6.11. IR (KBr): ν 3063.0 m, 2923.8 w, 2877.6 w, 1676.6 s, 1621.4 s, 1588.6 s, 1464.0 m, 1366.9 s, 1307.3 w, 1245.8 s, 1201.8 m, 1104.4 w, 1019.5 m, 814.4 m, 767.8 w, 690.6 w, 615.3 w, 436.4 w cm^{-1}. MS (FAB): *m*/*z* 412.5 [M$^+$ − Cl], 322.8 [M$^+$ − $MnCl_2$].

{**2-Acetyl-6-[1-((2,6-diisopropylphenyl)imino)ethyl]pyridine**}-**cobalt(II) Chloride (21)**. A 400 mg portion (1.24 mmol) of ligand **5** and 0.95 equiv of $CoCl_2$·6H_2O (280.6 mg) were dissolved in 10 mL of THF to give a green suspension, which was stirred for 14 h at room temperature. After addition of 20 mL of diethyl ether a precipitate was formed and was washed twice with 10 mL of diethyl ether. After drying in vacuo complex **21** was obtained in 400 mg (75%) yield. Crystals suitable for an X-ray analysis were obtained from a dichloromethane solution. Anal. Calcd for $C_{21}H_{26}N_2Cl_2CoO$ (452.28): C, 55.77; H, 5.79; N, 6.19. Found: C, 55.97; H, 5.85; N, 5.92. IR (KBr): ν 3081.3 m, 2956.9 s, 2924.4 m, 2867.4 m, 1675.9 s, 1588.6 s, 1462.1 s, 1442.3 m, 1366.5 s, 1310.2 m, 1248.1 s, 1094.3 m, 1056.1 m, 1025.0 s, 936.7 w, 818.1 s, 772.4 m, 691.9 w, 613.3 s, 440.0 w cm^{-1}. MS (FAB): *m*/*z* 415.9 [M$^+$ − Cl], 378.9 [M$^+$ − 2Cl], 323.0 [M$^+$ − $CoCl_2$], 306.9 [M$^+$ − ($CoCl_2$, Me)].

{**2-Acetyl-6-[1-(2,6-(diisopropylphenyl)imino)ethyl]pyridine**}-**nickel(II) Chloride (22a)**. A 200 mg portion (0.62 mmol) of ligand **5** and 0.98 equiv of $NiCl_2$·6H_2O (281 mg) were dissolved in 10 mL of THF to give a clear solution. After 10 min the mixture became cloudy. The solution was stirred for 14 h at 50 °C and was filtered afterward. The residue was extracted twice with 10 mL of DCM and dried in vacuo. Yield: 147 mg (54%). Anal. Calcd for $C_{21}H_{26}N_2Cl_2NiO$ (452.04): C, 55.80; H, 5.80; N, 6.20. Found: C, 55.22; H, 6.15; N, 5.88. IR (KBr): ν 3081.3 m, 2956.8 s, 2924.4 m, 2867.4 m, 1668.2 s, 1588.6 s, 1463.5 m, 1366.4 s, 1315.6 w, 1251.8 s, 1204.3 w, 1101.8 w, 1031.8 w, 818.3 s, 616.0 m cm^{-1}. MS (FAB): *m*/*z* 414.5 [M$^+$ − Cl], 379.7 [M$^+$ − 2Cl], 363.7 [M$^+$ − (2Cl, Me)].

{**2-Acetyl-6-[1-((2,6-diisopropylphenyl)imino)ethyl]pyridine**}-**nickel(II) Bromide (22b)**. The procedure was the same as for complex **22a**, except that (DME)$NiBr_2$ and as the solvent dichloromethane (20 mL) were used. The precipitate was washed twice

with 10 mL of toluene. Crystals suitable for an X-ray analysis were obtained from a saturated dichloromethane solution overlayered with *n*-pentane. Yield: 400 mg (96%). Anal. Calcd for $C_{21}H_{26}N_2Br_2NiO$ (540.95): C, 46.63; H, 4.84; N, 5.18. Found: C, 46.18; H, 4.73; N, 4.58. IR (KBr): ν 3065.7 m, 2969.7 s, 2919.8 m, 2860.1 m, 1673.3 s, 1616.7 w, 1591.9 s, 1458.8 m, 1370.0 m, 1312.6 w, 1250.4 m, 1057.7 m, 1029.9 m, 998.4 m, 811.8 s, 772.2 m, 742.5 m, 694.6 m, 612.5 m, 443.7 m cm^{-1}. MS (FAB): *m*/*z* 540.1 [M^+], 460.1 [$M^+ - Br$], 380.0 [$M^+ - 2Br$], 365 [$M^+ - (2Br, Me)$].

{**2-Acetyl-6-[1-((2,6-dimethylphenyl)imino)ethyl]pyridine**}-**nickel(II) Bromide (23)**. In a glovebox 225 mg (DME)$NiBr_2$ (0.73 mmol, 0.98 equiv) was dissolved in 10 mL of DCM and the suspension was stirred at room temperature. A 200 mg portion (0.75 mmol) of ligand **7** in 5 mL of DCM was added via canula. In the first 30 min the color changed to brown. The reaction mixture was stirred for 14 h at room temperature. The solvent was removed in vacuo, and the residue was washed twice with toluene (10 mL) and dried in vacuo. Yield: 325 mg (92%). Anal. Calcd for $C_{17}H_{18}N_2Br_2NiO$ (484.84): C, 42.11; H, 3.74; N, 5.78. Found: C, 41.78; H, 3.55; N, 5.70. IR (KBr): ν 3061.5 m, 2961.5 w, 2915.4 m, 2846.2 w, 1667.6 s, 1590.3 s, 1470.4 m, 1369.4 m, 1252.4 s, 1215.5 s, 1101.8 w, 1036.0 w, 810.7 w, 784.0 w, 741.9 w, 698.1 w, 618.5 w cm^{-1}. MS (FAB): *m*/*z* 484.5 [M^+], 404.6 [$M^+ - Br$], 324.7 [$M^+ - 2Br$], 309.7 [$M^+ - (2Br, Me)$].

{**2-Acetyl-6-[1-((2-isopropylphenyl)imino)ethyl]pyridine**}-**nickel(II) Bromide (24)**. The procedure was the same as for complex **23**. Complex **24** was obtained using 200 mg (0.71 mmol) of ligand **6** and 0.98 equiv of (DME)$NiBr_2$ (214.8 mg) in 88% yield (303 mg). Anal. Calcd for $C_{18}H_{20}N_2Br_2NiO$ (498.87): C, 43.34; H, 4.04; N, 5.62. Found: C, 43.78; H, 4.25; N, 6.00. IR (KBr): ν 3076.4 m, 2969.8 s, 2920.3 m, 1666.5 s, 1586.7 s, 1484.9 m, 1442.3 m, 1375.6 m, 1360.6 m, 1310.1 w, 1252.2 s, 1225.9 w, 1202.0 w, 1098.6 m, 1032.5 w, 815.7 m, 787.0 m, 668.4 m, 612.3 w, 496.3 w cm^{-1}. MS (FAB): *m*/*z* 498.6 [M^+], 418.7 [$M^+ - Br$], 338.8 [$M^+ - 2Br$], 323.8 [$M^+ - (2Br, Me)$].

Single-Crystal X-ray Structure Determination of Compounds 15, 18·CH_2Cl_2, 21·CH_2Cl_2, and 22b. Crystal data and details of the structure determination are presented in Table 3. Single crystals suitable for the X-ray diffraction study were grown by diffusion of *n*-pentane in saturated solutions of **15**, **18**, **21**, and **22b** in dichloromethane. A clear blue plate (purple needle, green needle, red fragment) was stored under perfluorinated ether, transferred to a Lindemann capillary, fixed, and sealed. Preliminary examination and data collection were carried out on area detecting systems (Stoe IPDS or Nonius Mach3, κ-CCD) at the window of a rotating anode (Nonius FR591) with graphite-monochromated Mo Kα radiation ($\lambda = 0.710\ 73$ Å). The unit cell parameters were obtained by full-matrix least-squares refinement of 43 241 (3909, 55 692, 58 666) reflections. Data collections were performed at 143 (173, 153, 153) K (Oxford Cryosystems) within a θ range of $1.83° < \theta < 26.20°$ ($2.81° < \theta < 25.60°$, $1.70° < \theta < 25.36°$, $2.33° < \theta < 25.38°$). A total number of 12 033 (4300, 9292, 8080) intensities were integrated. Raw data were corrected for Lorentz and polarization and, arising from the scaling procedure, for latent decay and absorption effects. After merging ($R_{int} = 0.020$ (0.103, 0.010, 0.027)) sums of 6247 (2234, 4744, 4148) (all data) and 5303 (1450, 4450, 4028) ($I > 2\sigma(I)$) respectively remained and all data were used. The structures were solved by a combination of direct methods and difference Fourier syntheses. All non-hydrogen atoms were refined with anisotropic displacement parameters. For **15**, **21**·CH_2Cl_2, and **22b**, all hydrogen atoms were found and refined with individual isotropic displacement parameters. For **18**·CH_2Cl_2, all hydrogen atoms were placed in calculated positions and refined using a riding model, with methylene and aromatic C−H distances of 1.00, 0.98, and 0.95 Å, respectively, and $U_{iso}(H) = 1.2[U_{eq}(C)]$ or $1.5[U_{eq}(C)]$. Full-matrix least-squares refinements with 460 (271, 383, 348) parameters were carried out by minimizing $\sum w(F_o^2 - F_c^2)^2$ with the Shelxl-97 weighting scheme and stopped at shift/error < 0.001. The final residual electron density maps showed no remarkable features. Neutral atom scattering factors for all atoms and anomalous dispersion corrections for the non-hydrogen atoms were taken from the International Tables for Crystallography. All calculations were performed on an Intel Pentium 4 PC, including the programs Platon, Sir92, and Shelxl-97.[51] For **15**, a problem with unresolvable solvent molecules in the unit cell was cured with the Platon calc squeeze procedure. For **18**·CH_2Cl_2, the relatively high *R* values and the low reflection count are the result of a very tiny crystal and severe twinning problems. **18**·CH_2Cl_2 is isostructural with **21**·CH_2Cl_2. For **22b**, the correct enantiomer is proved by Flack's parameter $\epsilon = 0.004(6)$. Crystallographic data (excluding structure factors) for the structures reported in this paper have been deposited with the Cambridge Crystallographic Data Center as Supplementary Publication Nos. CCDC-627692 (**15**), CCDC-627693 [**18**·(CH_2Cl_2)], CCDC-627694 [**21**·(CH_2Cl_2)], and CCDC-627695 (**22b**). Copies of the data can be obtained free of charge on application to the CCDC, 12 Union Road, Cambridge CB2 1EZ, UK (fax, (+44)1223-336-033; e-mail, deposit@ccdc.cam.ac.uk).

Acknowledgment. This work was generously supported by the Deutsche Forschungsgemeinschaft and the Bayerische Forschungsverbund Katalyse FORKAT and by NanoCat, an International Graduate Program within the Elitenetzwerk Bayern (postdoctoral fellowship to G.D.F.).

Supporting Information Available: CIF files, additional figures, and tables of crystallographic data, atomic coordinates, atomic displacement parameters, bond distances, and bond angles for complexes **15**, **18**·CH_2Cl_2, **21**·CH_2Cl_2, and **22b** and tables giving details of the oligomerization/polymerization results. This material is available free of charge via the Internet at http://pubs.acs.org.

OM060857Q

(51) (a) IPDS Operating System, Version 2.8; Stoe&Cie GmbH, Darmstadt, Germany, 1997**.** (b) Data Collection Software for Nonius *k*-CCD devices; Enraf-Nonius, Delft, The Netherlands, 2001. (c) Otwinowski, Z.; Minor, W. *Methods Enzymol.* **1997**, *276*, 307ff. (d) Altomare, A.; Cascarano, G.; Giacovazzo, C.; Guagliardi, A.; Burla, M. C.; Polidori, G.; Camalli, M. SIR92. *J. Appl. Crystallogr*. **1994**, *27*, 435. (e) *International Tables for Crystallography*; Wilson, A. J. C., Ed.; Kluwer Academic: Dordrecht, The Netherlands, 1992; Vol. C, Tables 6 .1.1.4, 4.2.6.8, and 4.2.4.2. (f) Spek, A. L. PLATON, A Multipurpose Crystallographic Tool; Utrecht University, Utrecht, The Netherlands, 2005. (g) Sheldrick, G. M. SHELXL-97; Universität Göttingen, Göttingen, Germany, 1998.